Observables, Measurements, Sensors, Platforms, and Models

Marcello G. Magaldi

IR0000032 – ITINERIS, Italian Integrated Environmental Research Infrastructures System
(D.D. n. 130/2022 - CUP B53C22002150006) Funded by EU - Next Generation EU PNRR-Mission 4 “Education and Research” - Component 2: “From research to business” - Investment 3.1: “Fund for the realisation of an integrated system of research and innovation infrastructures”

Finanziato dall'Unione europea NextGenerationEU
Ministero dell'Università e della Ricerca
Italiadomani

Objectives

- Provide evidence of the complexity of circulation models
- Focus more on the what models can do rather than explain the intricate model mechanisms
- Barely considering blending and data assimilation examples
- No data driven method, no AI

Numerical circulation models

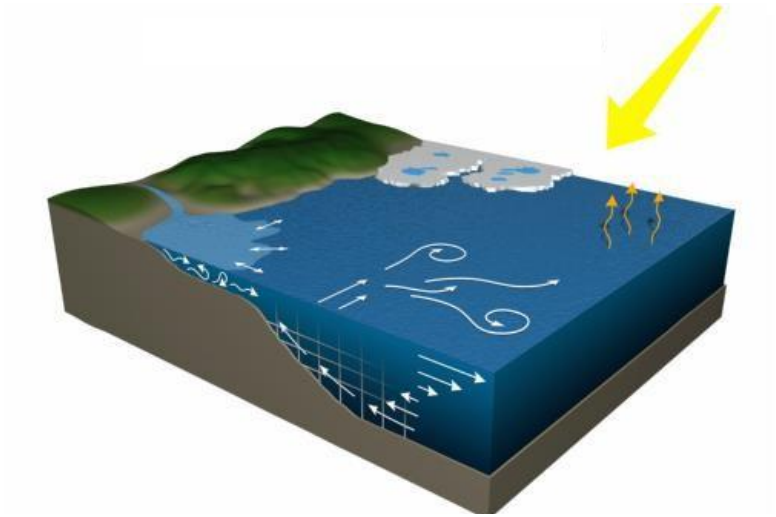

The COMET Program
Mesoscale Ocean Circulation Models

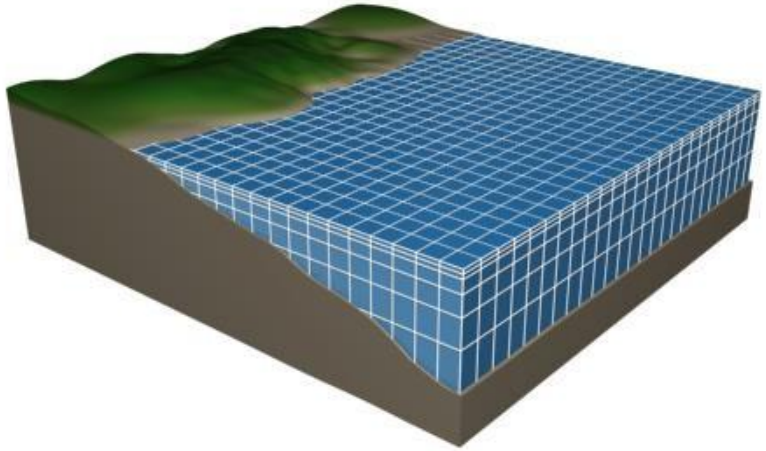

$$
\begin{cases}
\dfrac{d\rho}{dt} = -\rho\,\boldsymbol{\partial}\cdot\mathbf{v} + q_m & \text{Continuity eq.} \\
\dfrac{d\mathbf{v}}{dt} = -\dfrac{1}{\rho}\boldsymbol{\partial}\,p - \boldsymbol{\partial}\,\Phi - 2\boldsymbol{\Omega}\wedge\mathbf{v} + \dfrac{1}{\rho}\boldsymbol{\partial}\cdot\mathcal{T} & \text{Momentum eq.} \\
\dfrac{dT}{dt} = \boldsymbol{\partial}\cdot(\kappa_T\boldsymbol{\partial}\,T) + \dfrac{q_c}{\rho c_V} & \text{Temperature eq.} \\
\dfrac{dS}{dt} = \boldsymbol{\partial}\cdot(\kappa_S\boldsymbol{\partial}\,S) + \dfrac{q_s}{\rho} & \text{Salinity eq.} \\
\rho = \rho(p,T,S) & \text{Eq. of state}
\end{cases}
$$

Ocean circulation models consider a set of differential equations based on the laws of physics and fluid dynamics. The equations are solved over a specific area that is divided into ("discretized" with) a three-dimensional numerical grid. At each point on this grid, variables such as current velocities, temperature and salinity are calculated.

Vertical discretization

https://www.oc.nps.edu

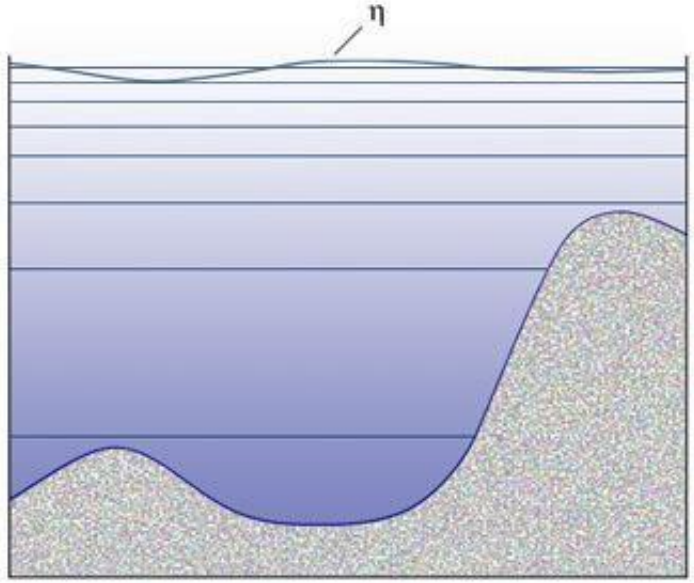

z-models

The vertical coordinate is depth, or "z"

Pros: simplest system perfect for areas that are well-mixed because they can provide the very fine resolution needed to represent three-dimensional turbulent processes

Cons: fixed number of depth levels in the ocean, problems in regions of sloping topography. Increasing the number of vertical levels will improve the representation of the near-bottom flow, but at a high computational cost

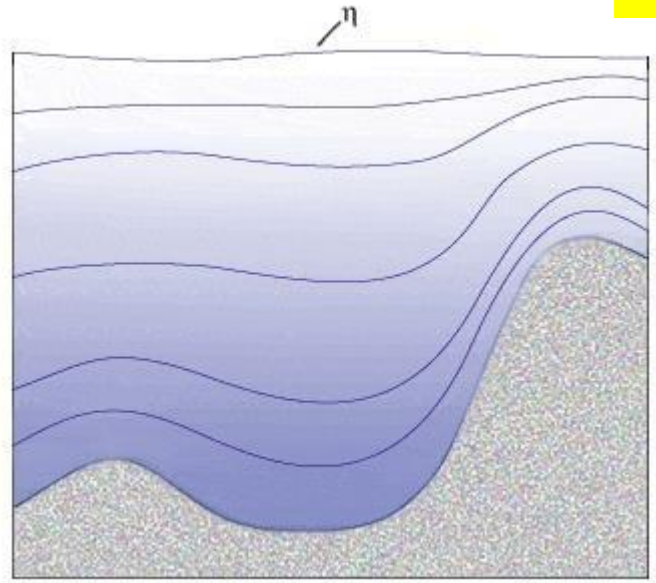

sigma- (or σ-)models

The vertical coordinate follows the bathymetry ("terrain following")

Pros: same number of vertical grid points everywhere in the domain, no matter how deep the water column. Levels could be clustered near the surface and/or bottom for better resolution of the the boundary layers

Cons: difficulty in handling sharp topographic changes. Pressure-gradient errors can give rise to unrealistic flows. Increasing resolutions helps mitigate this problem.

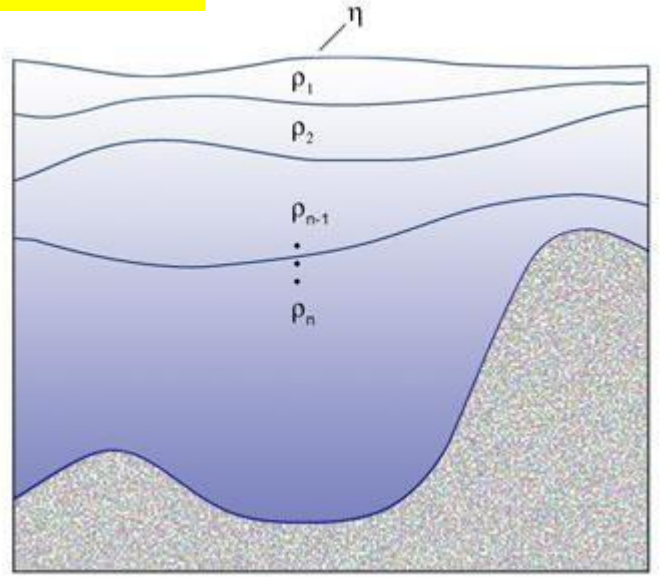

isopycnal or layered models

The vertical coordinate is the potential density referenced to a given pressure.

Pros: This system is more natural as it divides the water column into distinct homogeneous layers, whose thicknesses can vary from place to place and from one time step to the next. It works well for modeling tracer transport, which tends to be along surfaces of constant density.

Cons: difficulty in handling well mixed areas where important mixing processes take place

Horizontal discretization

Structured grid

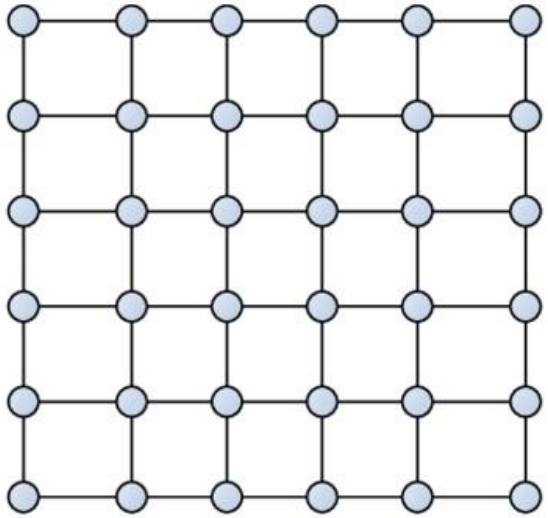

Unstructured grid

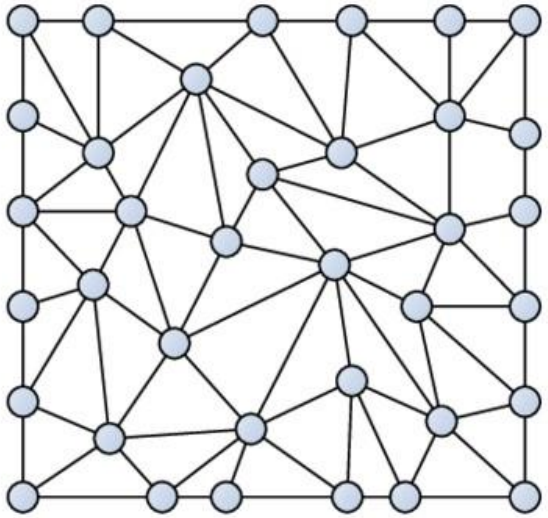

Roughly speaking, in structured meshes the nodes and vertices are regularly placed, and there is no need of additional information in order to locate. In unstructured meshes the nodes and vertices may be placed in an irregular manner according to the geometry of the specific case. In unstructured meshes you must keep arrays with information about nodes localization (coordinates) and nodes connectivity to build the elements, but complex geometries are better represented than in the structured cases.

The ROMS Arakawa-C grid

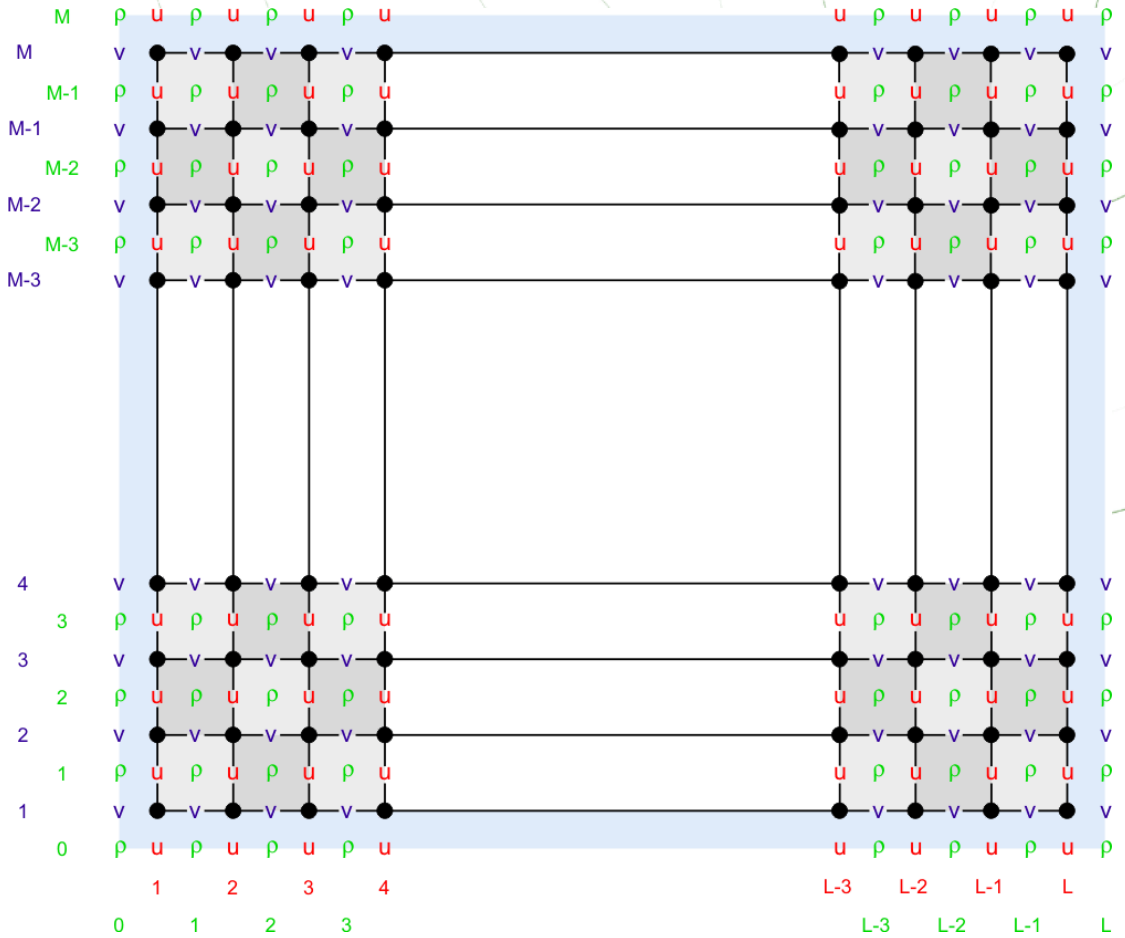

Ligurian Integrated Modelling Effort: LIME-ROMS

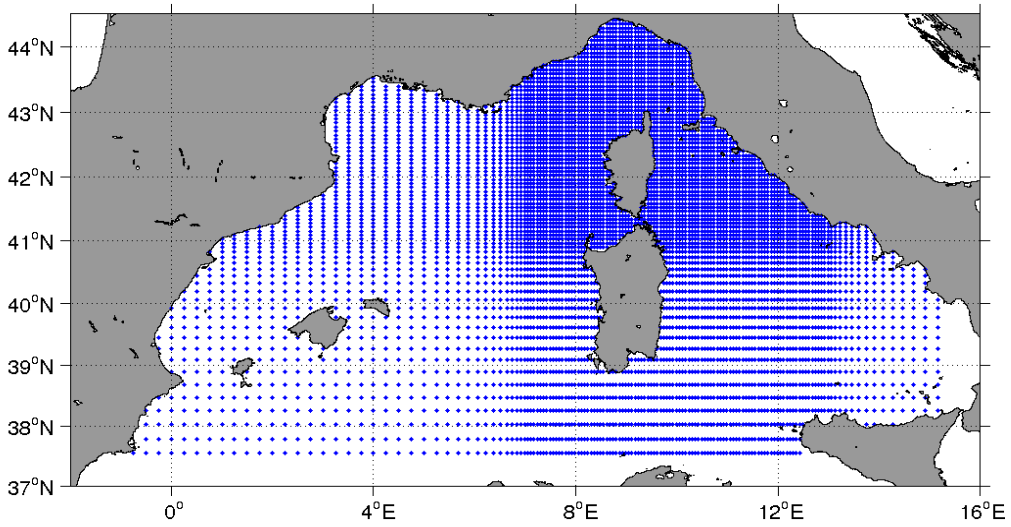

Simulated years	2004-2006
Min Horizontal resolution	1/16 x 1/16 (~ 6 km)
Max Horizontal resolution	1/64 x 1/64 (~1.5 km)
Vertical Coordinates	Sigma (50 levels)
Surface Forcing	ERA-INTERIM (3 hourly)
Boundary Condition	Mediterranean Forecasting System-SYS4a3 product (daily)
Bathymetry	ETOPO1

Telescopic grid: high-resolution in the Northern Tyrrhenian and Ligurian Seas

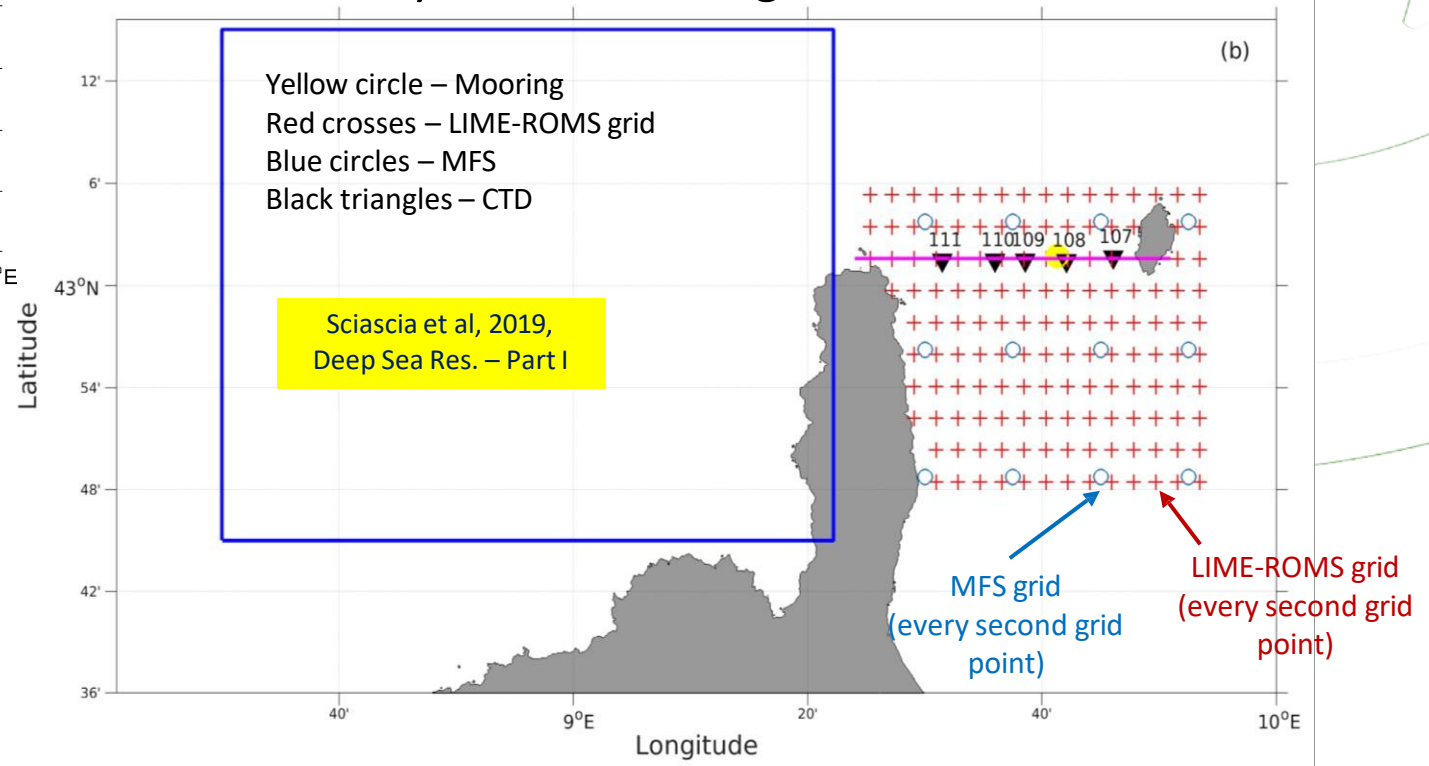

Corsica Channel Transect

Sciascia et al, 2019, Deep Sea Res. – Part I

LIW → Levantine Intermediate Water

MAW → Modified Atlantic Water

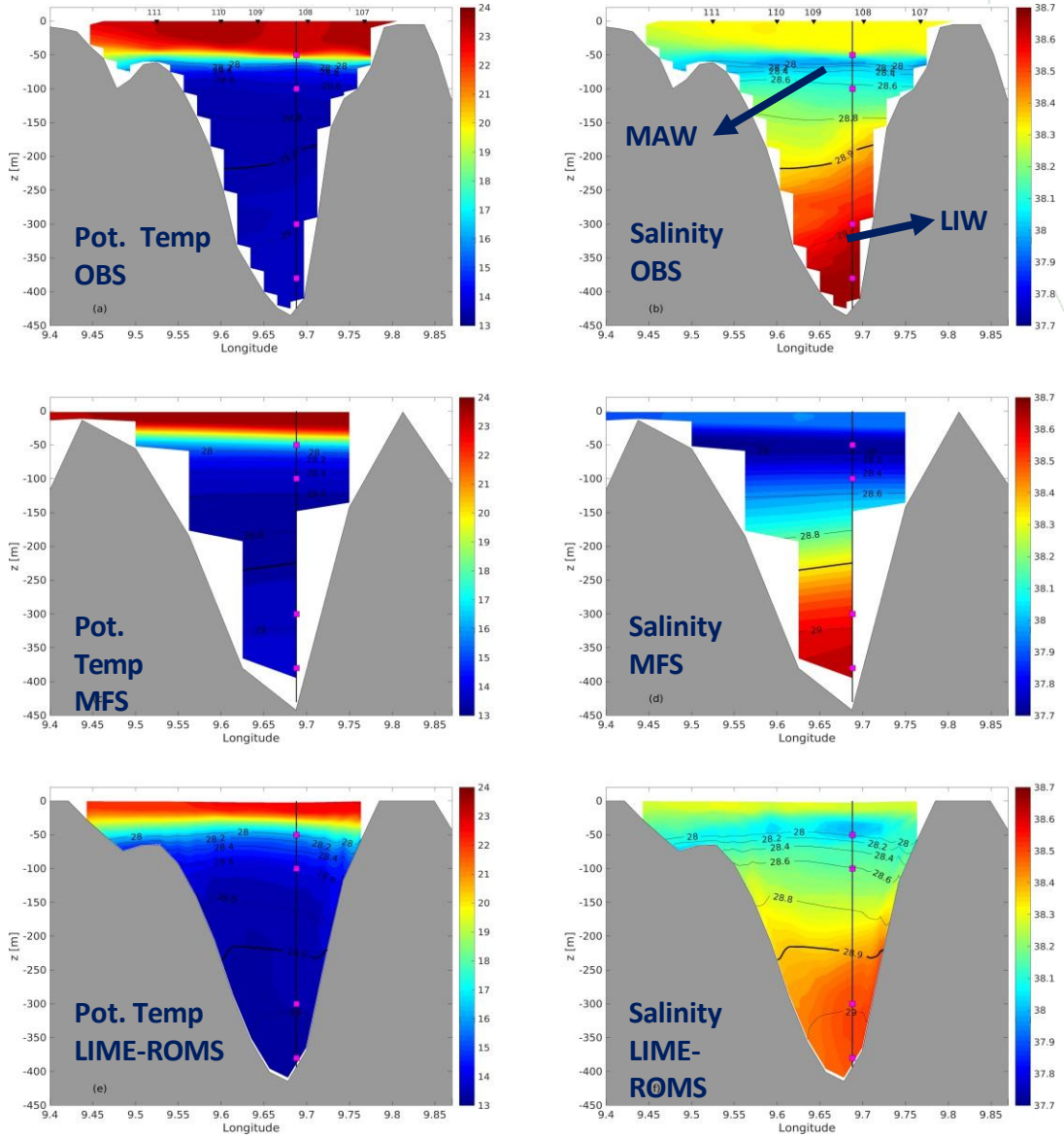

MFSTEP1 campaign, transect in the Corsica Channel on 24 September 2004

- Hydrography of both models (MFS and LIME-ROMS) in line with observations
- Levantine Intermediate waters simulated by MFS are closer to observations
- Surface salinity of LIME-ROMS agrees better with observations than MFS

Transport values

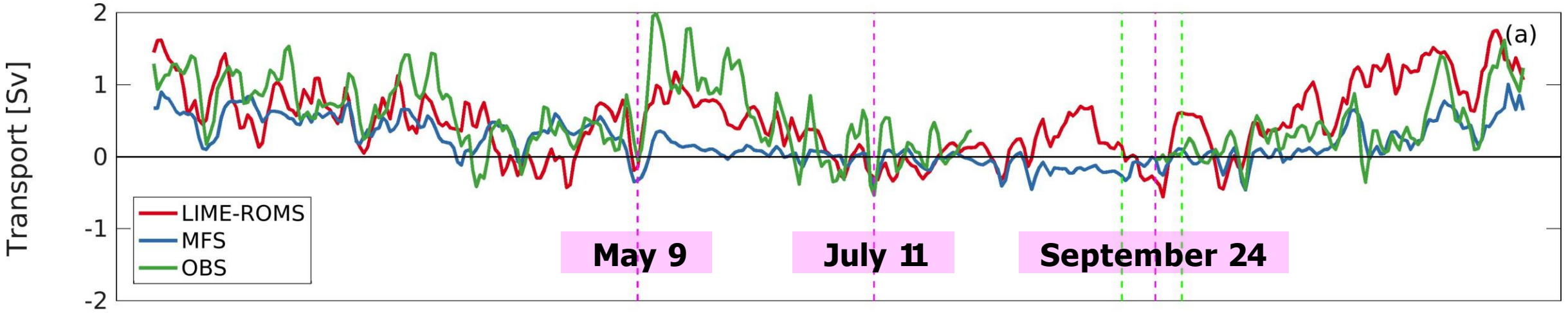

LIME-ROMS	0.49 ± 0.49 Sv	(0.53 ± 0.49 Sv)
MFS	0.19 ± 0.30 Sv	(0.25 ± 0.28 Sv)
OBS	0.54 ± 0.50 Sv	

Sciascia et al, 2019, Deep Sea Res. – Part I

- Numerical transport values comparable to observations
- Higher variability for the high-resolution model

Comparison to currentmeters (rotors)

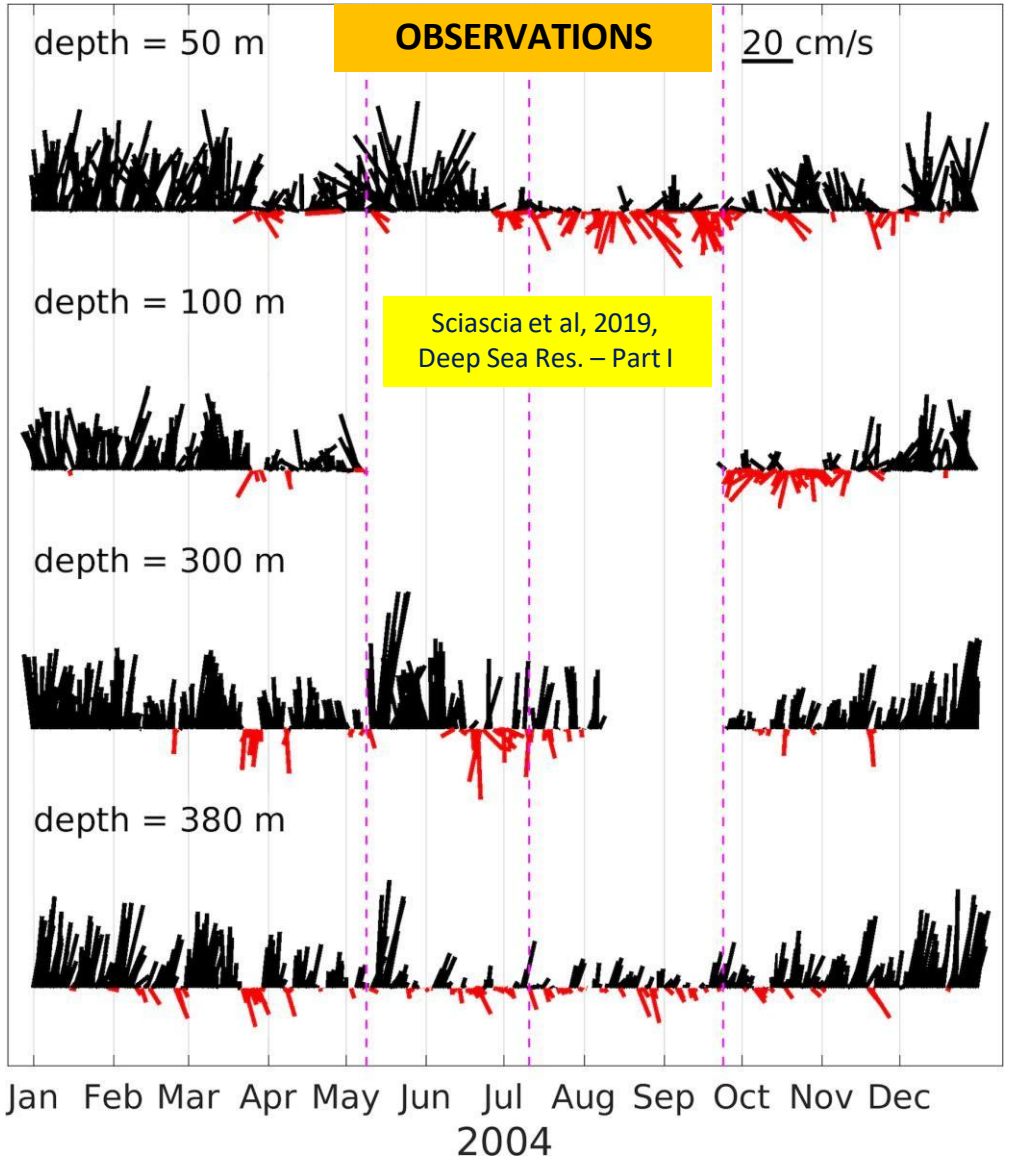

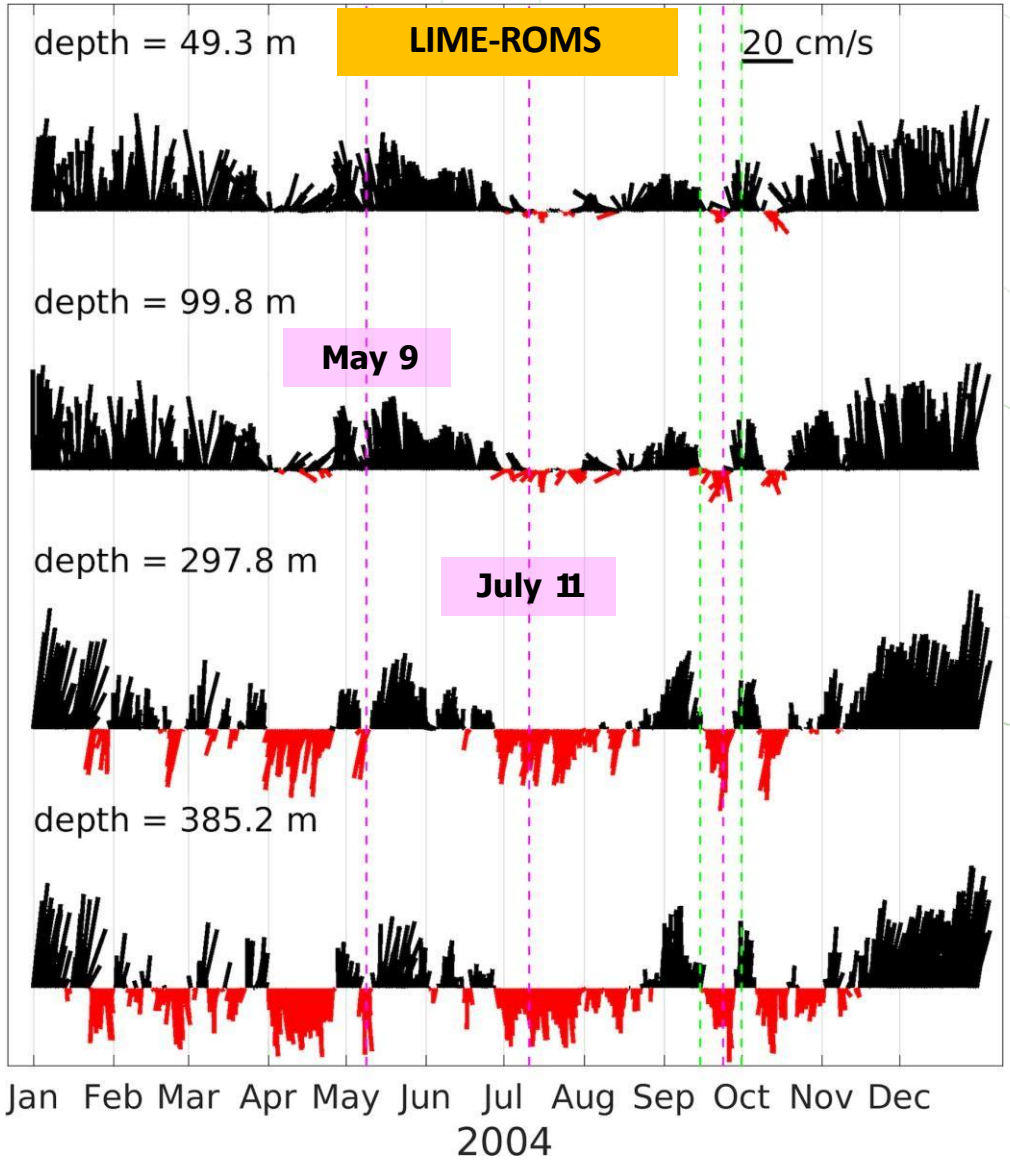

- Good agreement between observations and model
- Maximum velocity at depth
- Current inversions during the year

Single mooring in the Channel

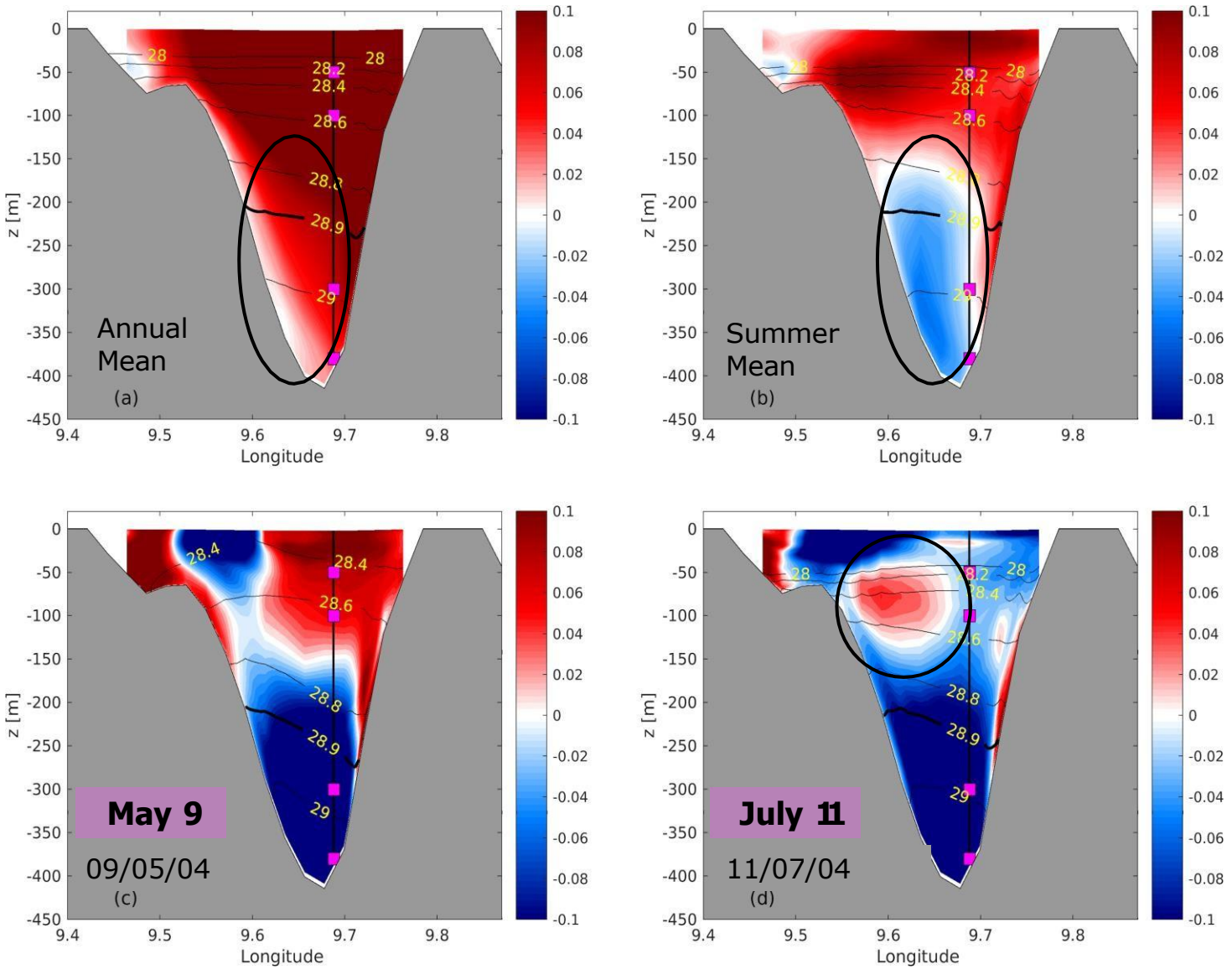

Is a single mooring enough to resolve the high-variability of the current in the Channel and its inversions?

- Annual means of the meridional velocities are northward (positive) and almost uniform across the whole Channel
- In some portions of the Channel, seasonal and daily southward (negative) velocities are observed

Turbulent nature of the flow

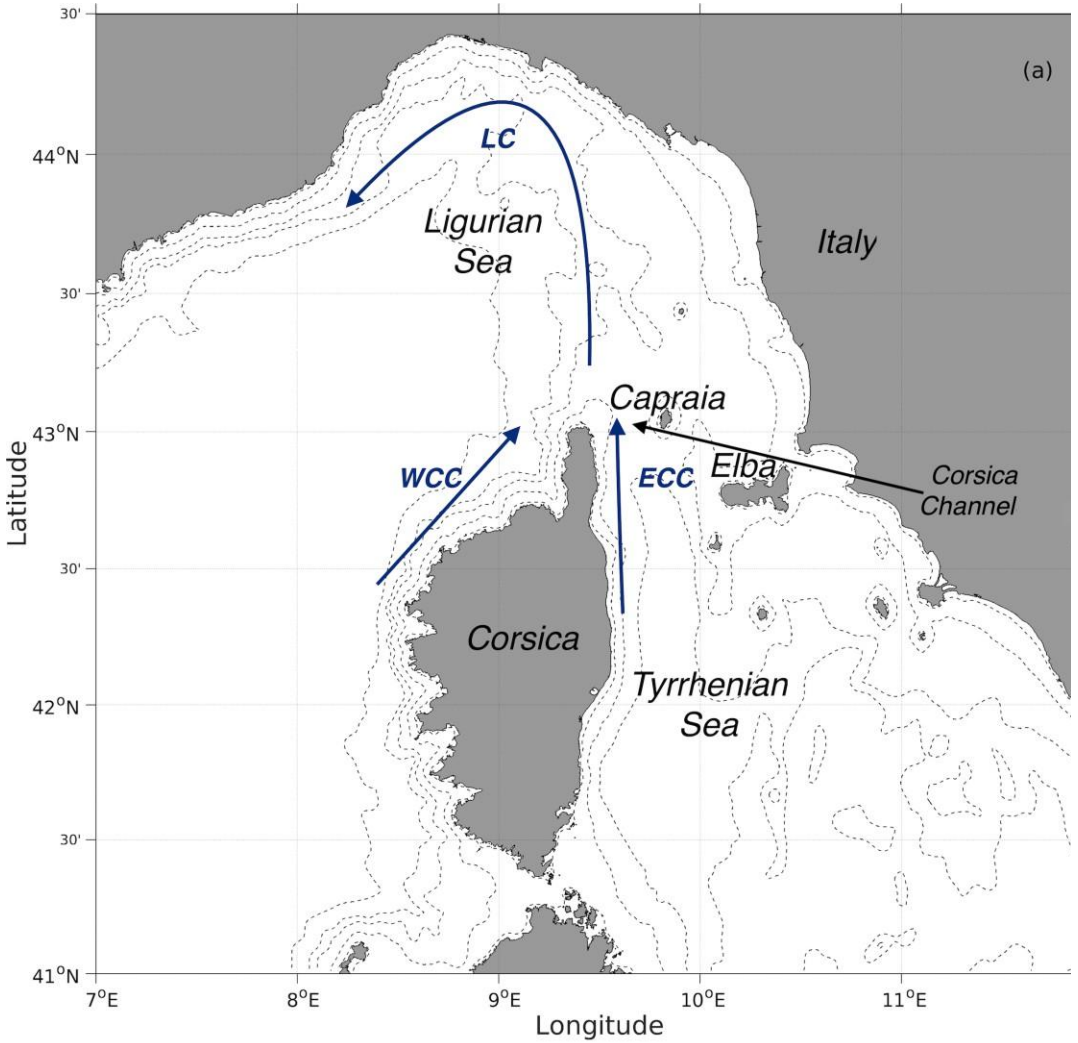

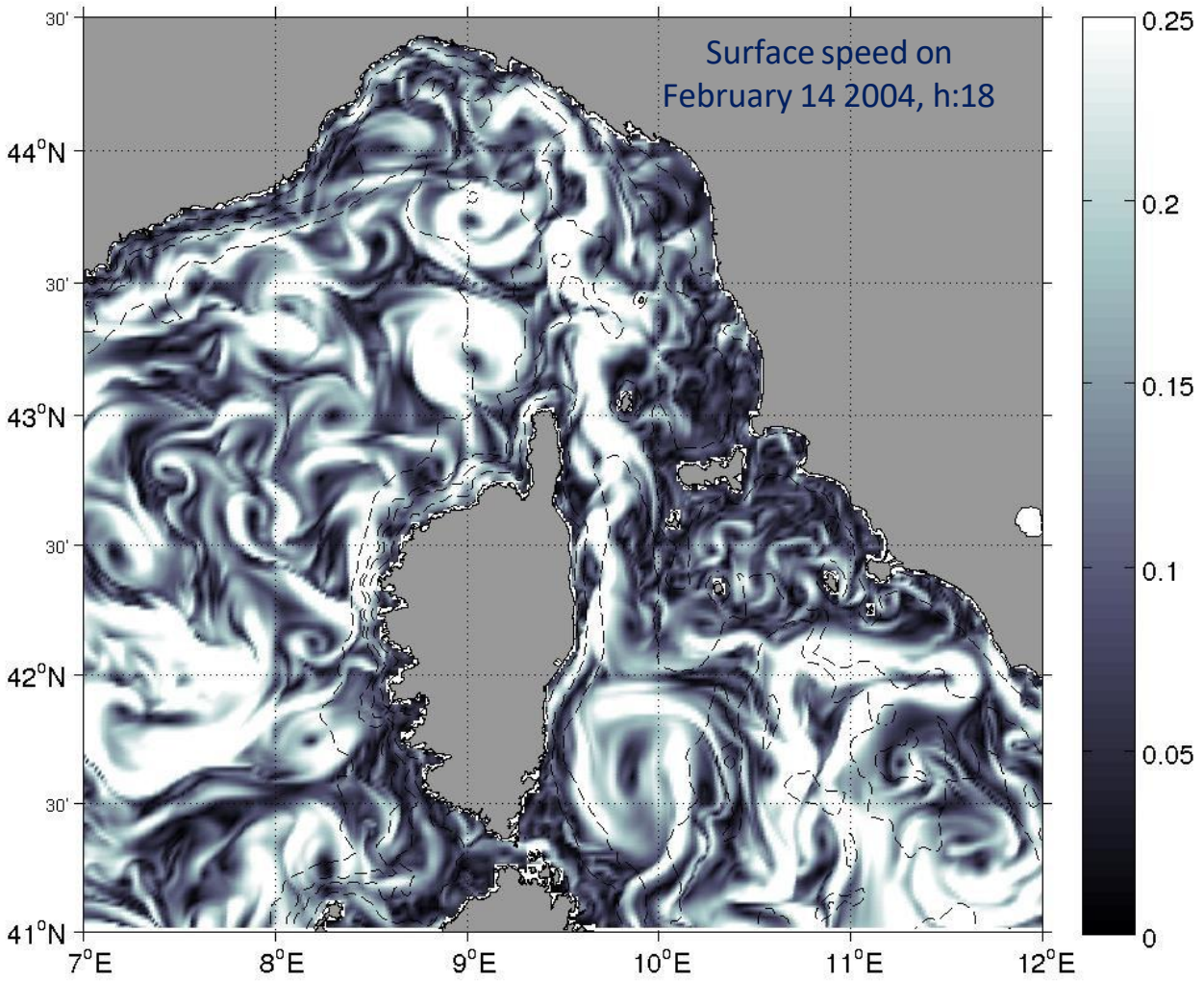

Circulation composite scenarios

Sciascia et al, 2019,
Deep Sea Res. – Part I

Composite pictures obtained averaging all instances when inversions (negative transport values) or normal conditions (positive values) are registered

Depth: 300m

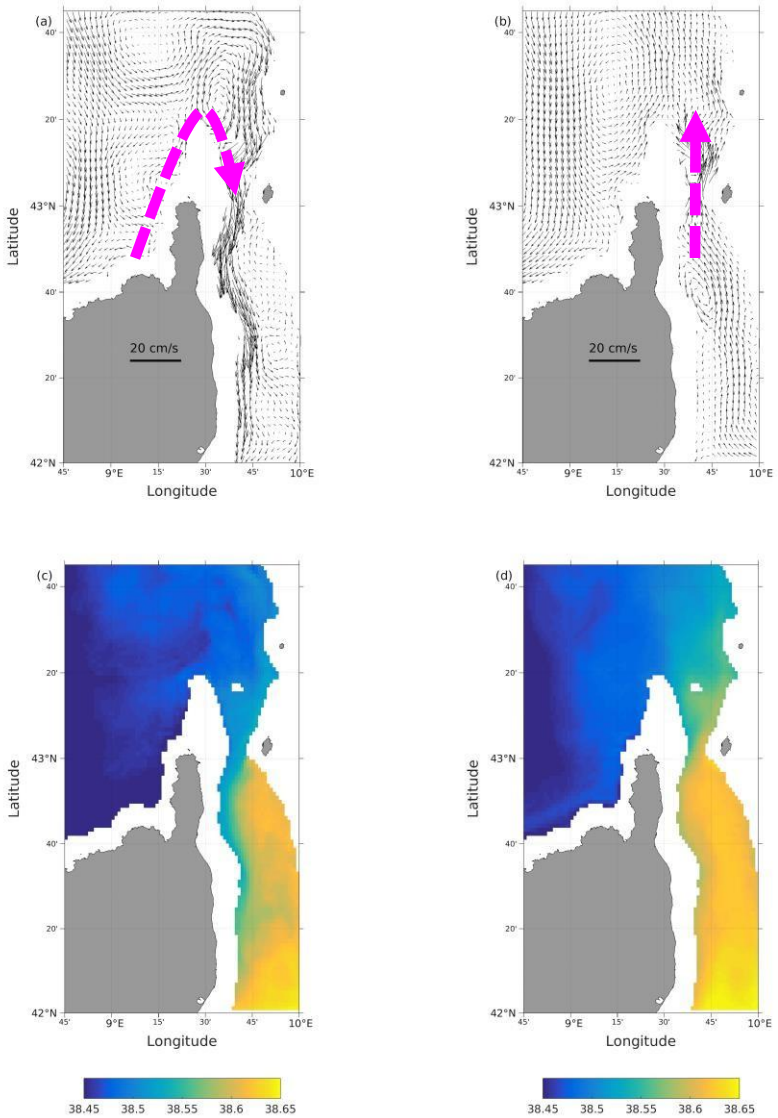

- **Scenario 1 "Current inversion":** the WCC veers rapidly on the right, it enters the Corsica Channel and keeps moving southward carrying Atlantic-origin waters which are colder and fresher. The ECC with warmer and saltier waters is stopped and remains on the eastern flank of the Channel

- **Scenario 2 "Normality"**: the ECC move northward bringing levantine waters, warmer and fresher, into the Ligurian SeaMar Ligure

Other evidences for the inversions

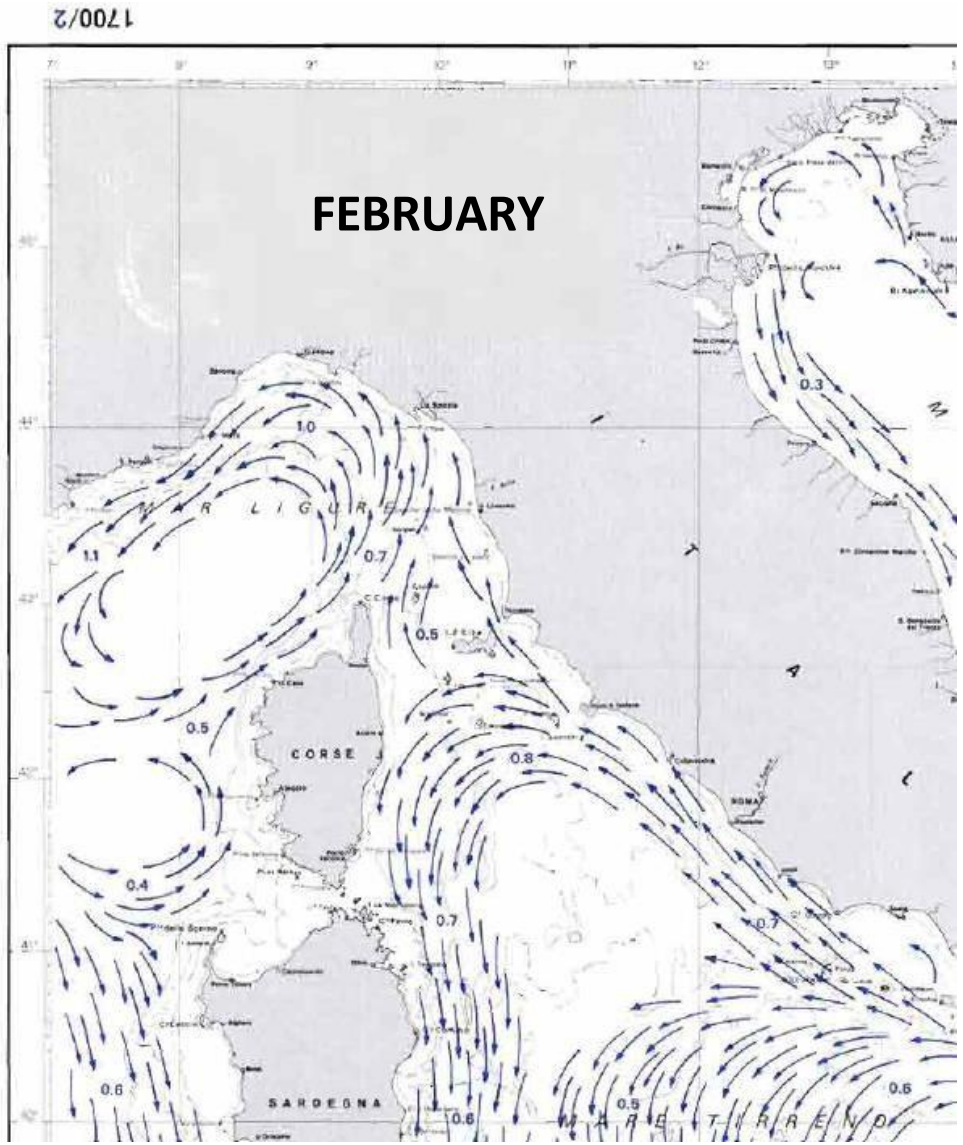

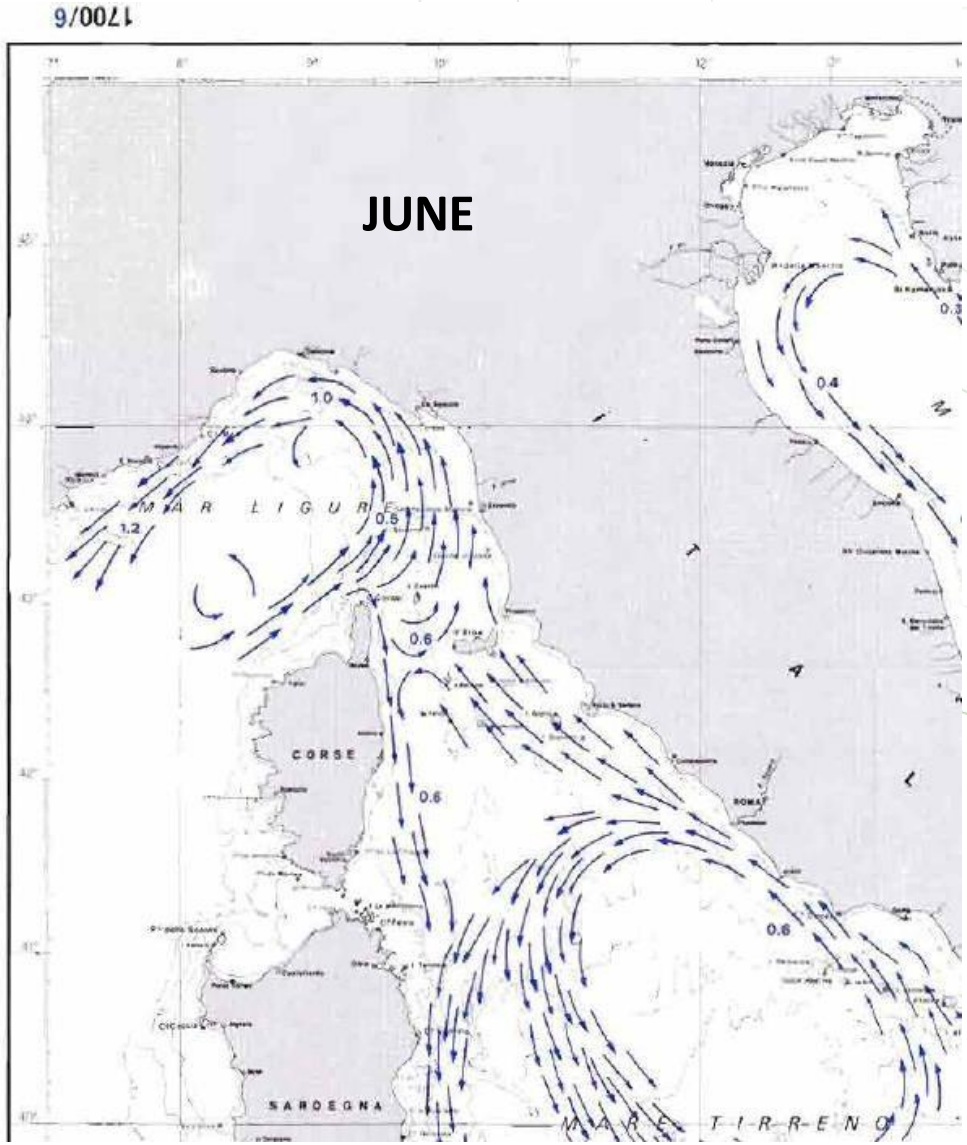

Atlas of the surface currents of the Italian Seas

Hydrographic Office of the Italian Navy Genoa, 1982

Stocchino's inversions

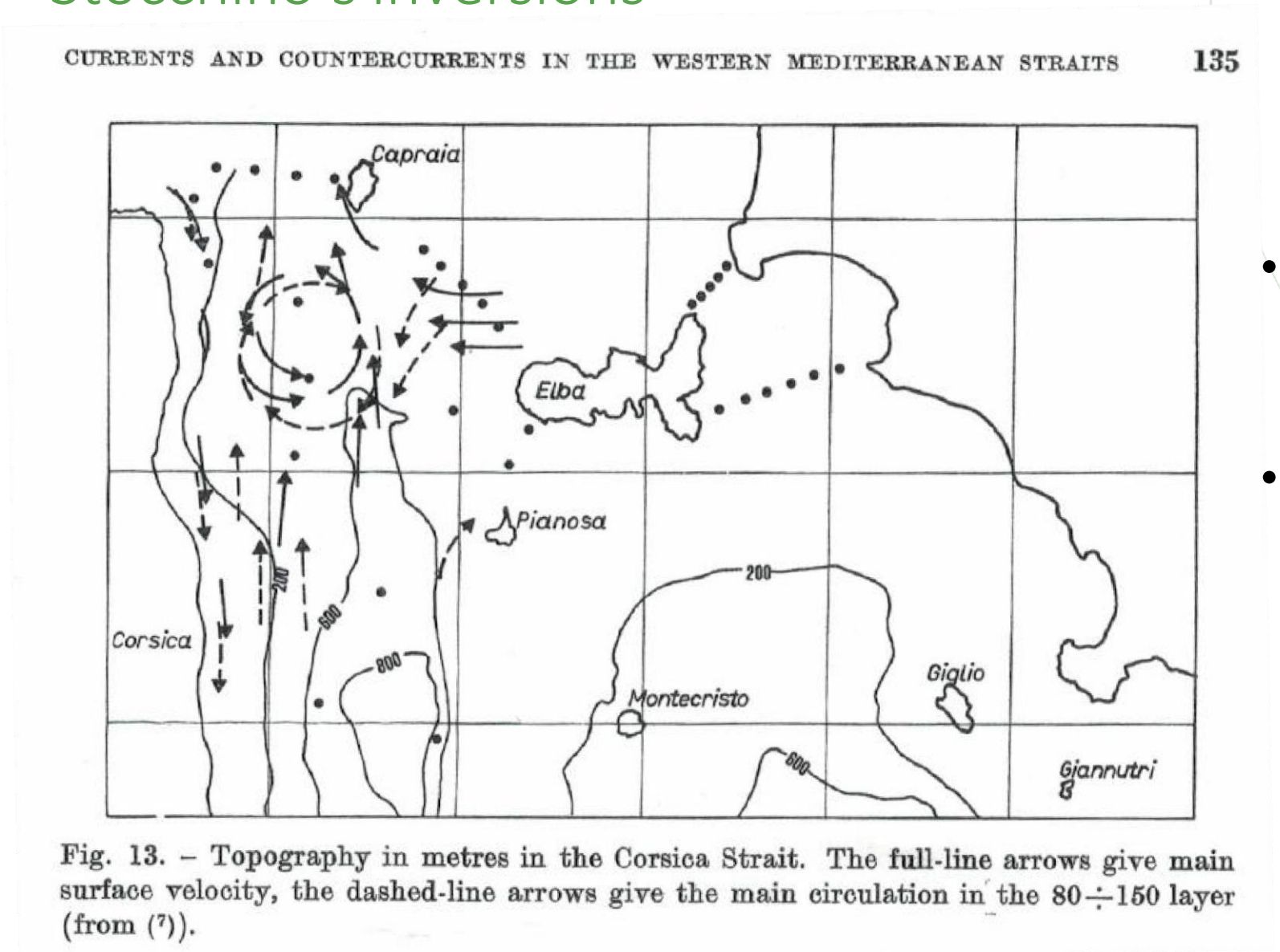
CURRENTS AND COUNTERCURRENTS IN THE WESTERN MEDITERRANEAN STRAITS 135

Fig. 13. – Topography in metres in the Corsica Strait. The full-line arrows give main surface velocity, the dashed-line arrows give the main circulation in the 80÷150 layer (from (7)).

- Firstly observed by Stocchino and Testoni (1966) and since then neglected
- Reproposed by Colacino et al. (1981) and by Sallusti and Travaglioni (1985) to show evidences of dynamical countercurrents in the straits

Where the glaciers meet the ocean

What is the role of the ocean in melting glaciers?

Straneo et al, 2010

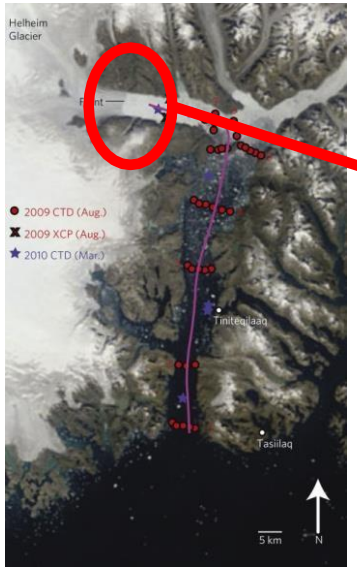

Relative high temperatures observed underneath the glaciers

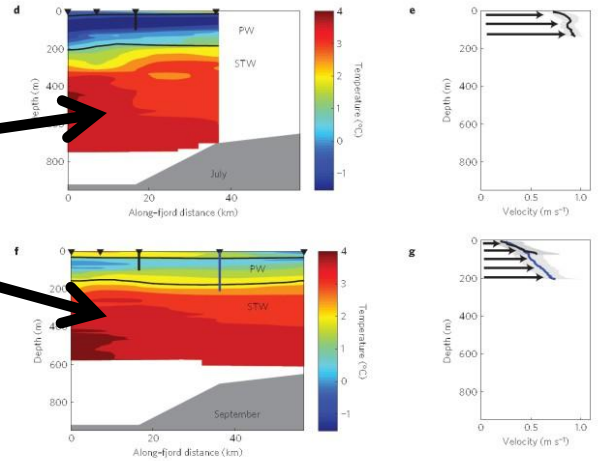

Figure 2 | Measurements in Sermilik Fjord in summer 2008 and the three water masses, GM, PW and STW. a, Potential temperature in July (blu
September (red). **b**, Salinity (colours as **a**). **c**, Potential temperature versus salinity (colours as **a**). Potential-density contours are overlaid in black (t
lines are $\sigma_\theta = 20$ and 25 kg m^{-3}). **d**,**f**, Potential-temperature distribution in the along-fjord direction ($x = 0$ is the mouth) from across-section averag
July and September, respectively. The 31.5 and 34 isohalines are overlaid to separate the three layers. Top triangles indicate section location and ver
bars the velocity sections. Bathymetry is shaded in grey. **e**,**g**, Along-fjord velocity averaged across fjord at the sections indicated in **d** and **f**, respecti
positive is towards the head of the fjord. Shading indicates the standard deviation across the section; arrows indicate the direction of flow.

Irminger Sea

Magaldi et al, 2011
J. Phys. Oceanogr.

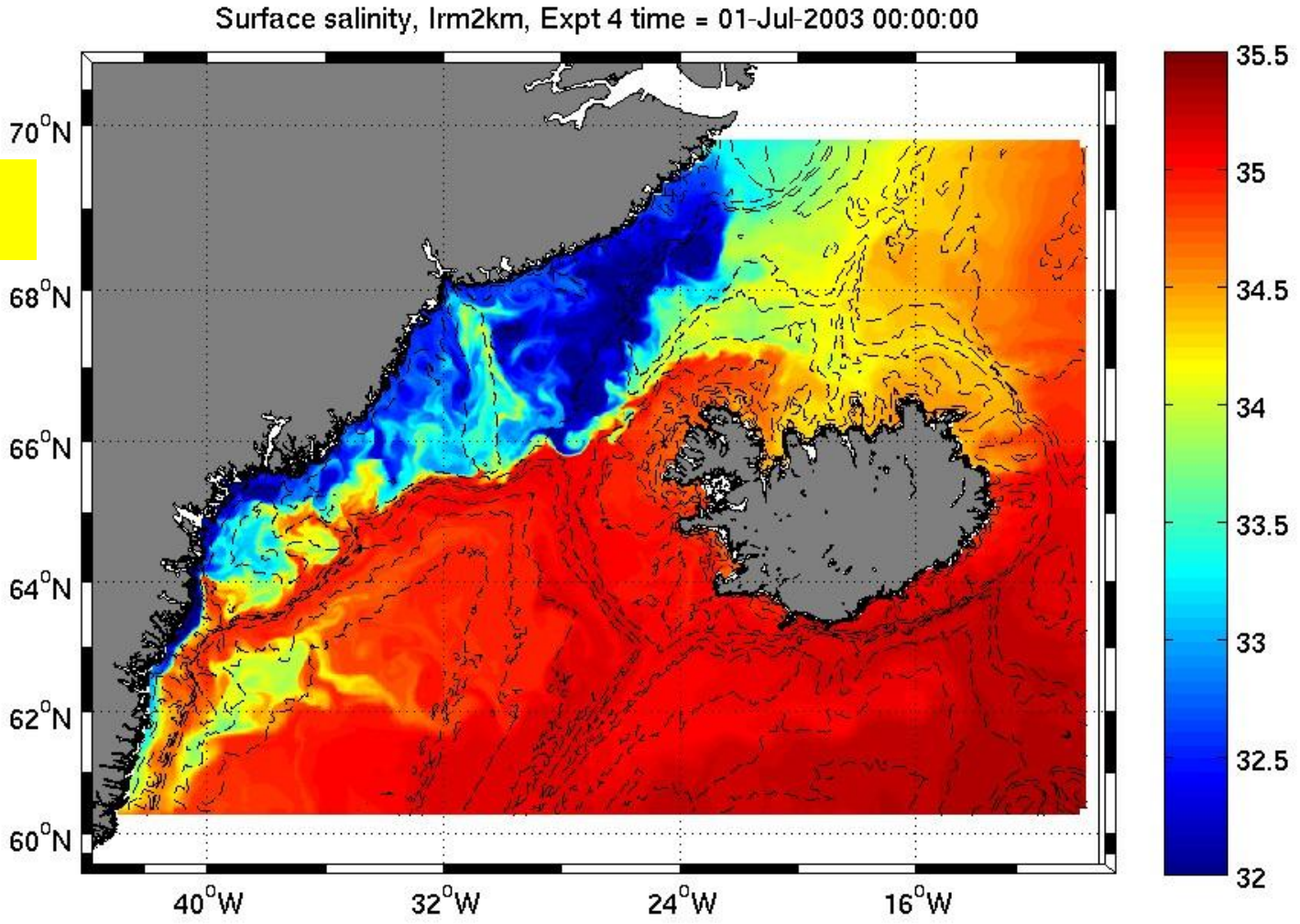

Numerical simulations to study small-scale processes and their influence influencing on the mixing of different water masses

Oceanic role

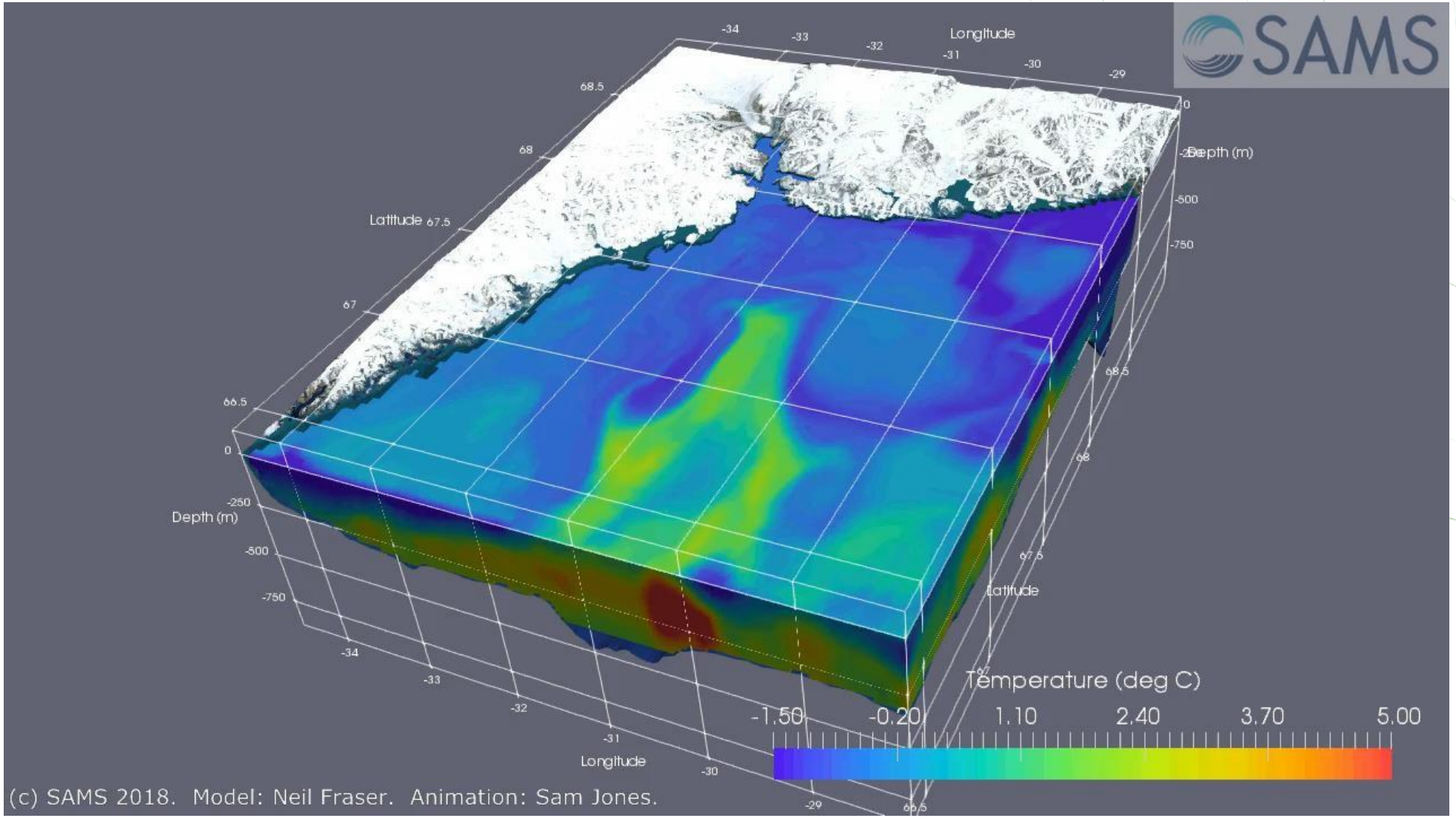

Fraser et al, 2018
J. Geophys. Res.

Data assimilation

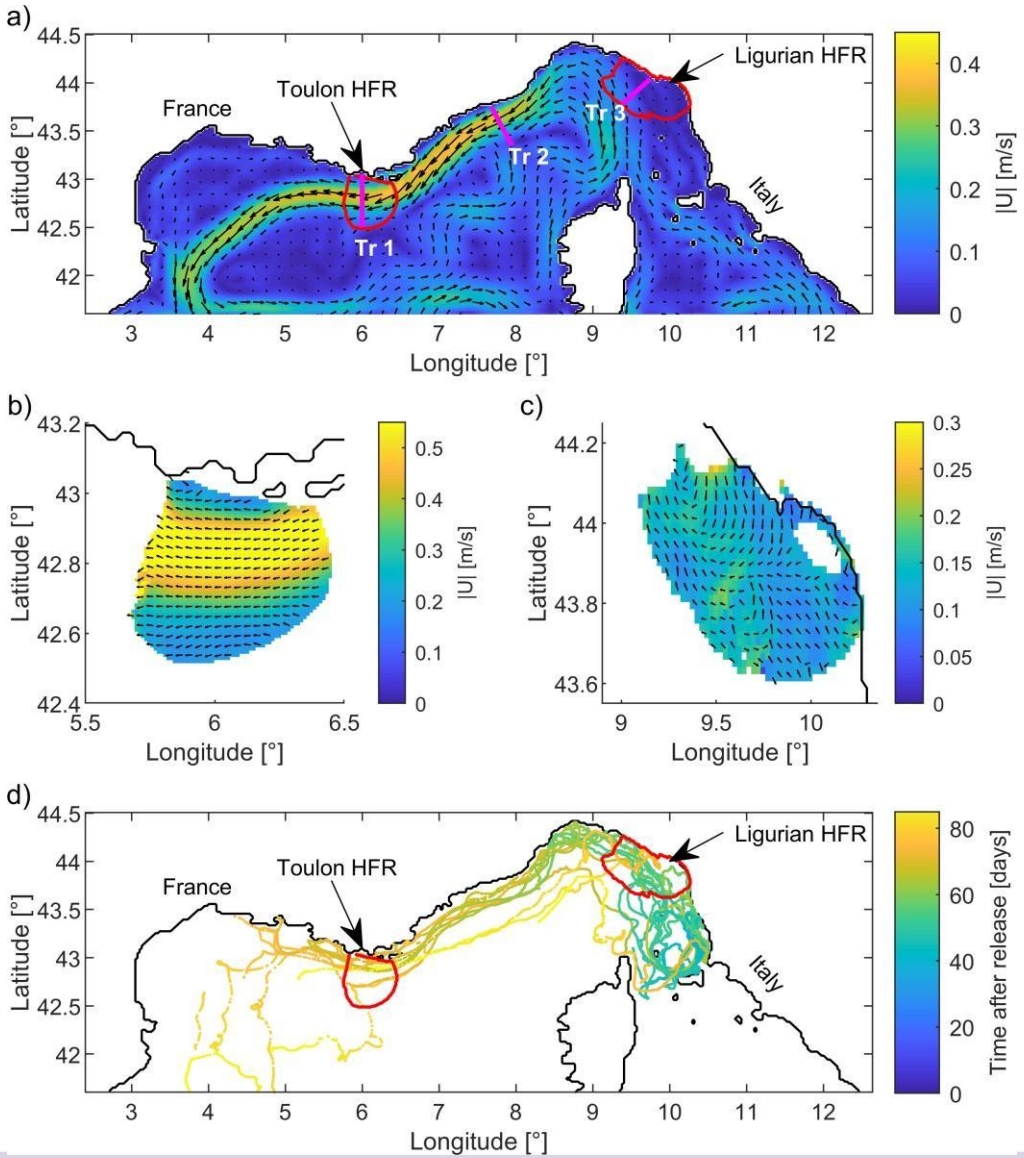

Numerical domain

Bendoni et al, 2023, Oc. Modell.

Assimlated observations (HF-Radar, SST)

Independent observations (drifters) for DA validation

- ROMS 4D-Var
- Δx ~ 2.2 km
- 3 months
- Assimilation window: 3 days
- Initial and boundary conditions: NEMO
- Atmospheric forcings: IFS-ECMWF

Taylor diagrams

Bendoni et al, 2023, Oc. Modell.

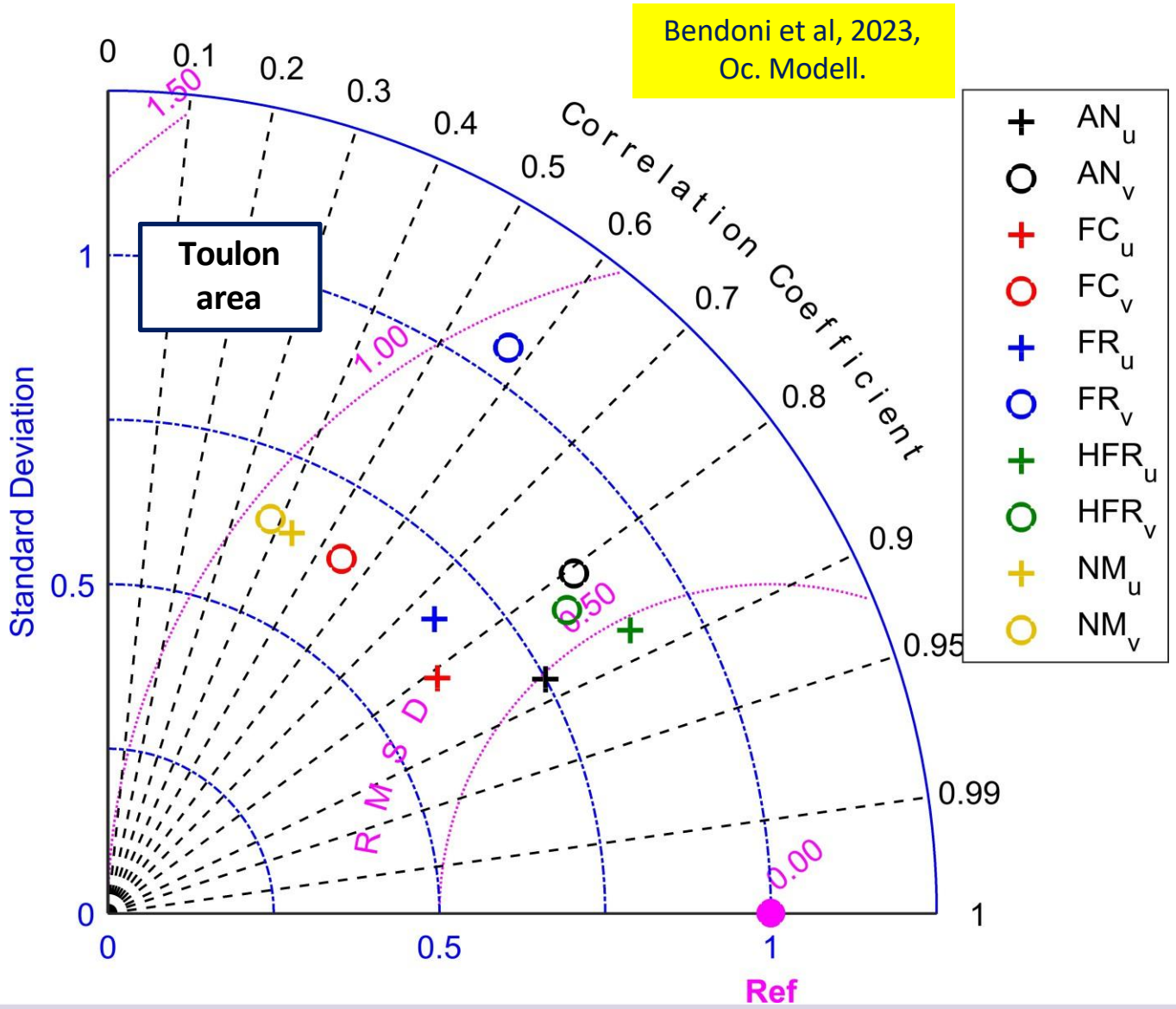

- Drifters are assumed to be the truth
- Differences between different observations (drifters and HF radars)
- 3-day assimilation windows (Analysis) followed by Forecast
- Comparison with Freerun model (without DA) and with NEMO
- DA improves surface dynamics inside HF-radar areas both for the Analysis and the Forecast if compared with the Freerun and NEMO
- Error reduction and the correlation increase are larger for the Analysis than for the Forecast

Coastal buoyant flow

Salinity increases offshore to mimic riverine water

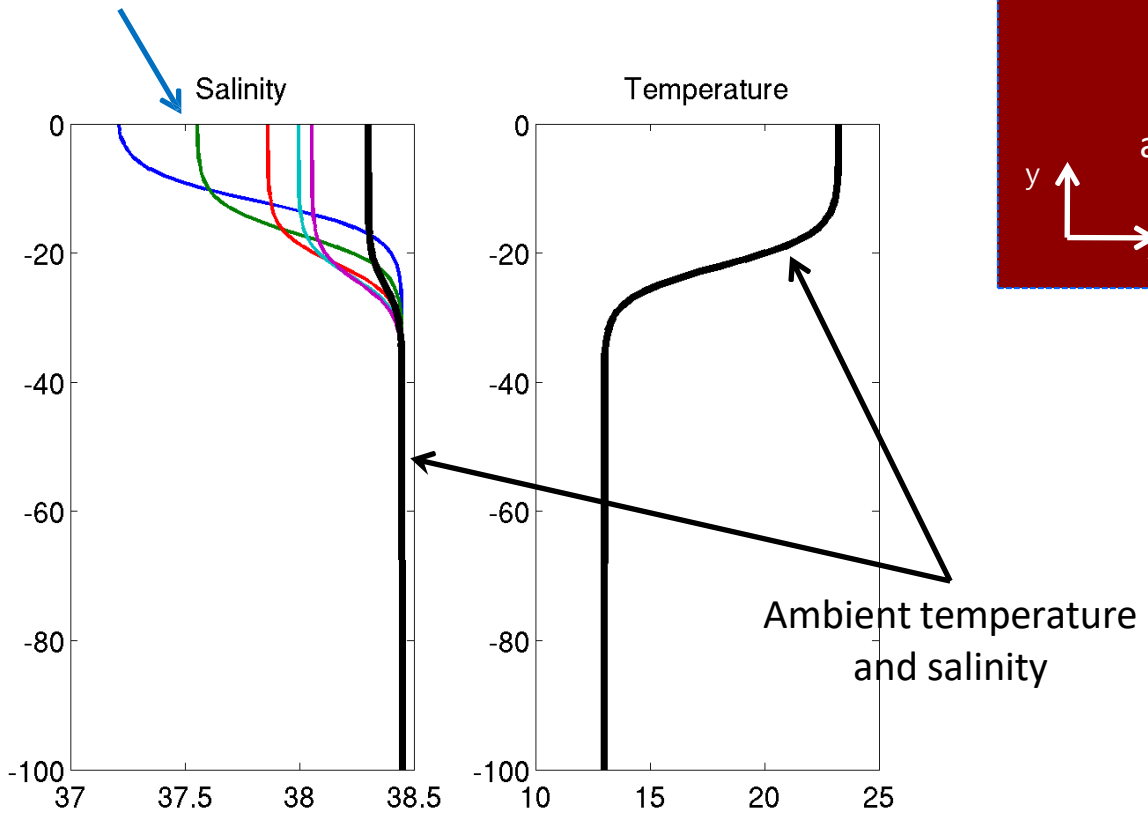

ROMS: Regional Ocean Modeling System

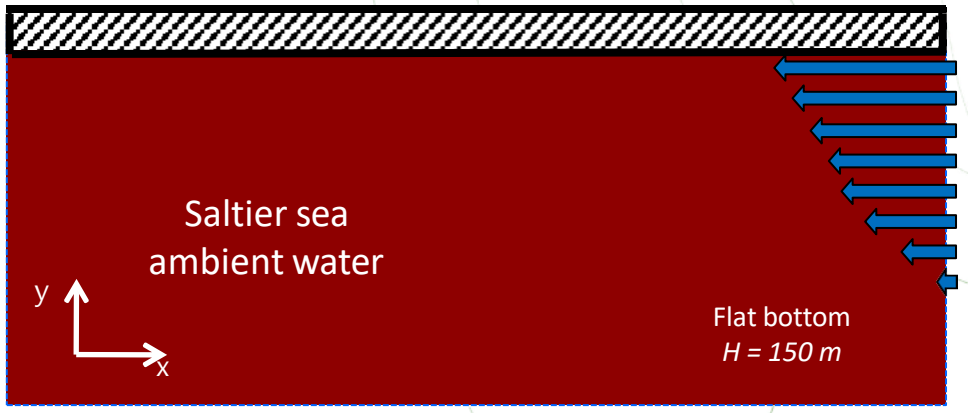

Mainly forced by salinity conditions at the eastern boundary

$$u_E(y,z) = \int_{-H}^{z} \frac{\partial u}{\partial z} dz = \frac{g}{f\rho_o} \int_{-H}^{z} \frac{\partial \rho}{\partial y} dz,$$

$$U_E(y) = \frac{1}{H} \int_{-H}^{0} u_E(y,z) dz,$$

$$\eta_E(y) = \eta_S - \frac{f}{g} \int_{0}^{y} U_E(y) dy,$$

Coastal buoyant flow

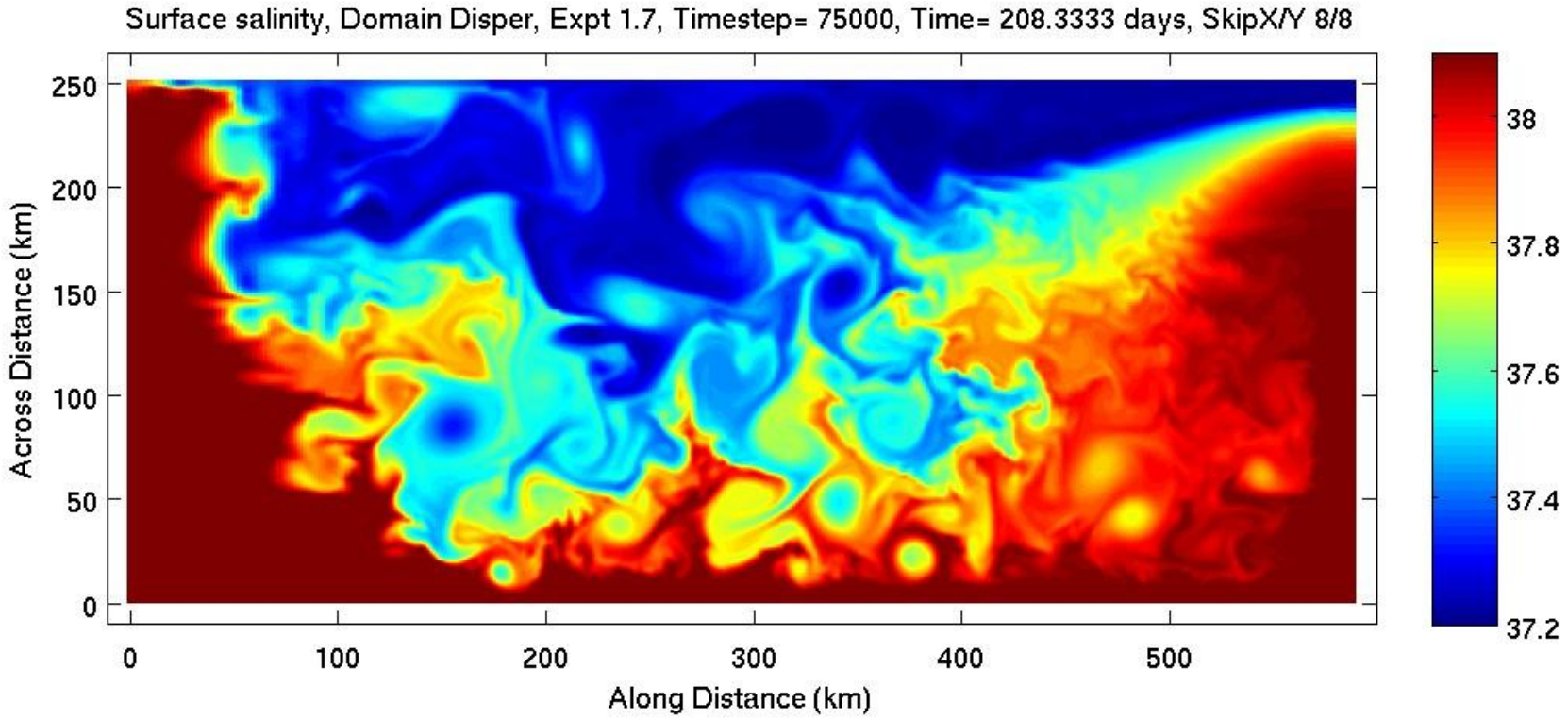

Poje et al, 2010, Ocean Modell.

Different resolutions

Synthetic drifter release

Each quintuplet is 12.5 km apart

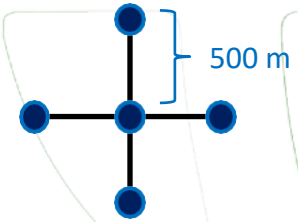

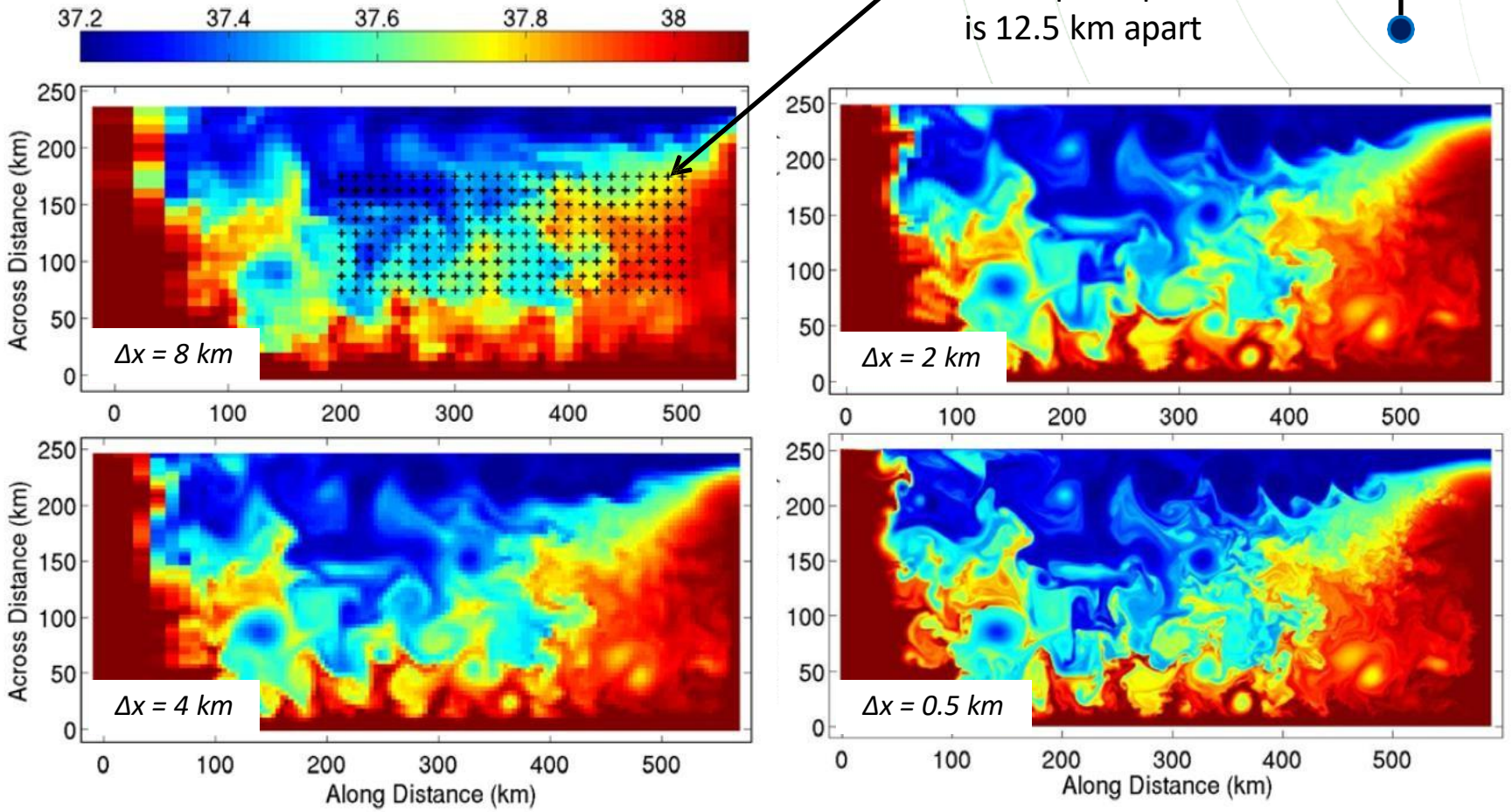

Finite Scale Lyapunov Exponent

FSLEs are a measure of dispersion of particles in a turbulent flow and consist of averages in times at fixed distances

$$\lambda(\delta) = \ln(\alpha)\left\langle \frac{1}{T(\delta)} \right\rangle$$

T is the averaged time (over the number of particle pairs) required to separate from a distance of δ to $\alpha\delta$

$$D(t) = D(0)\exp^{\lambda t} \qquad \lambda = \ln\left(\frac{D(\tau)}{D(0)}\right)\frac{1}{\tau}$$

Strength of exponential plateau increases with increasing resolutions

Poje et al, 2010, Ocean Modell.

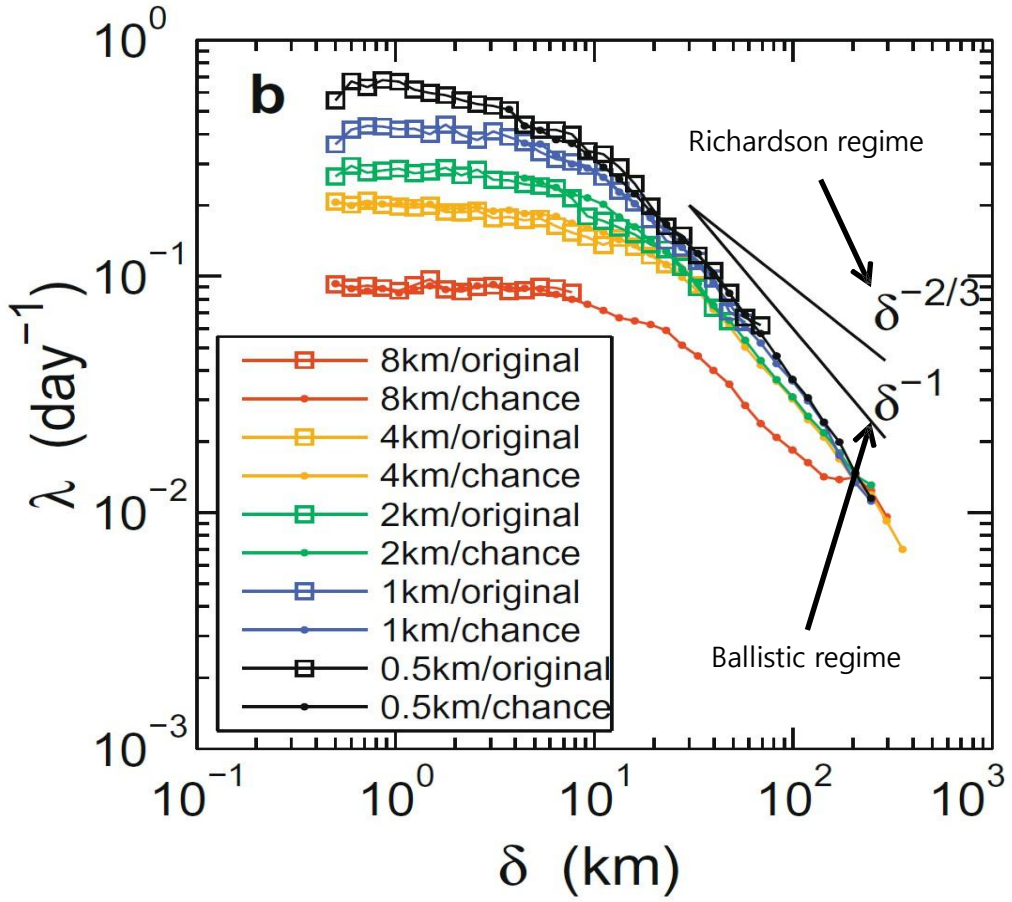

Turbulent structures and dispersion in the Ligurian Sea

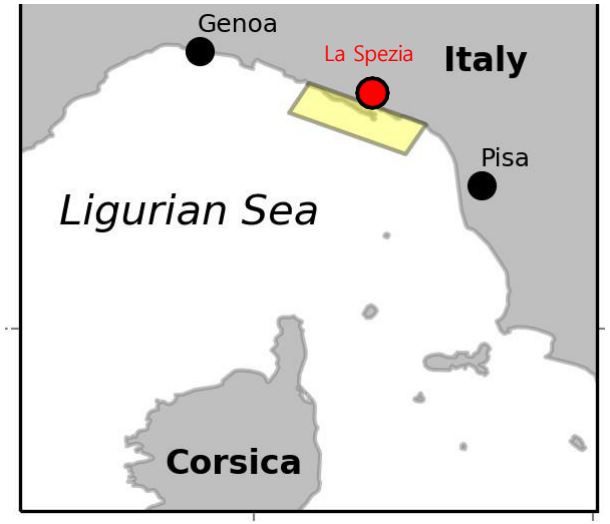

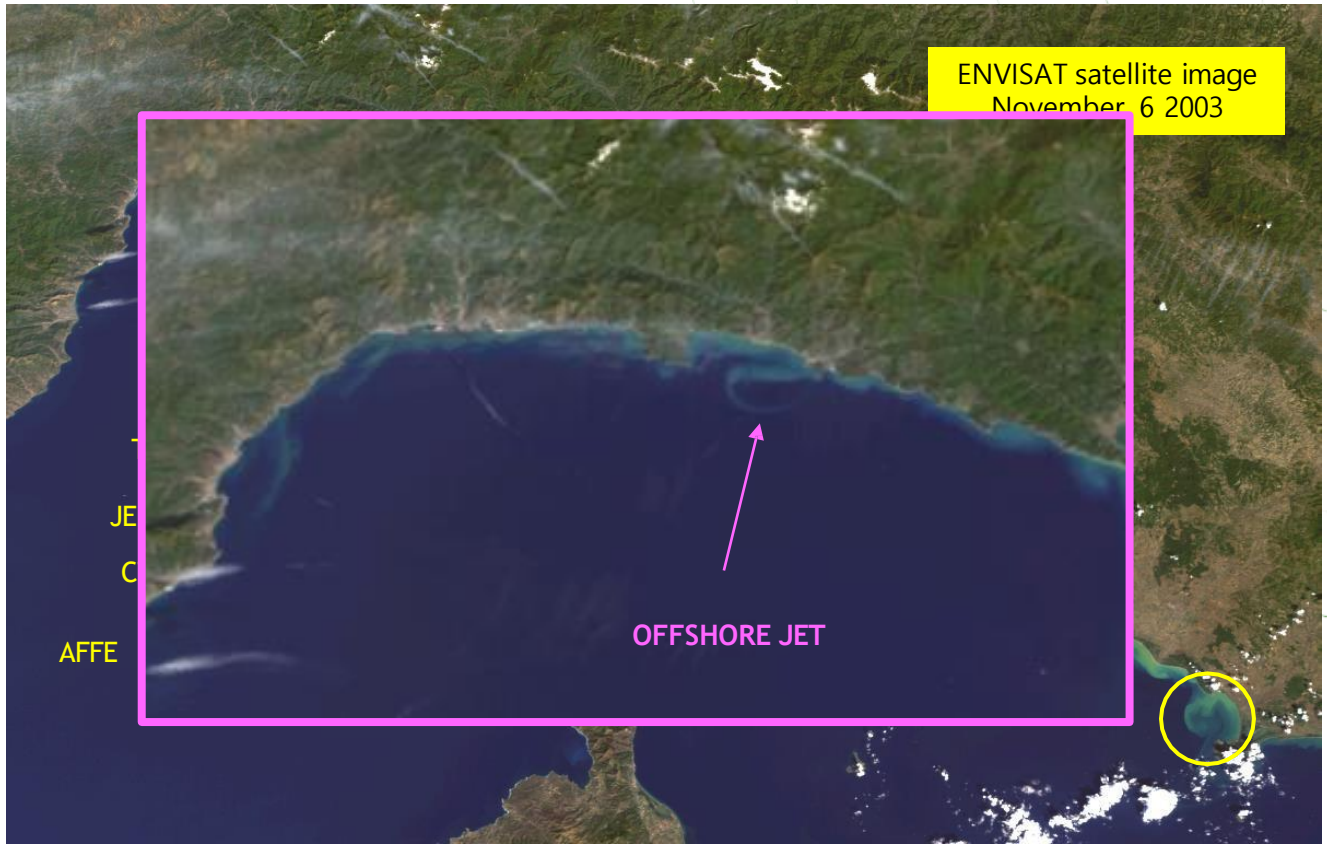

Current direction and square capes

Courtesy of Dr. Mattia Almansi, Ph.D. at Johns Hopkins University
Now at B-Open

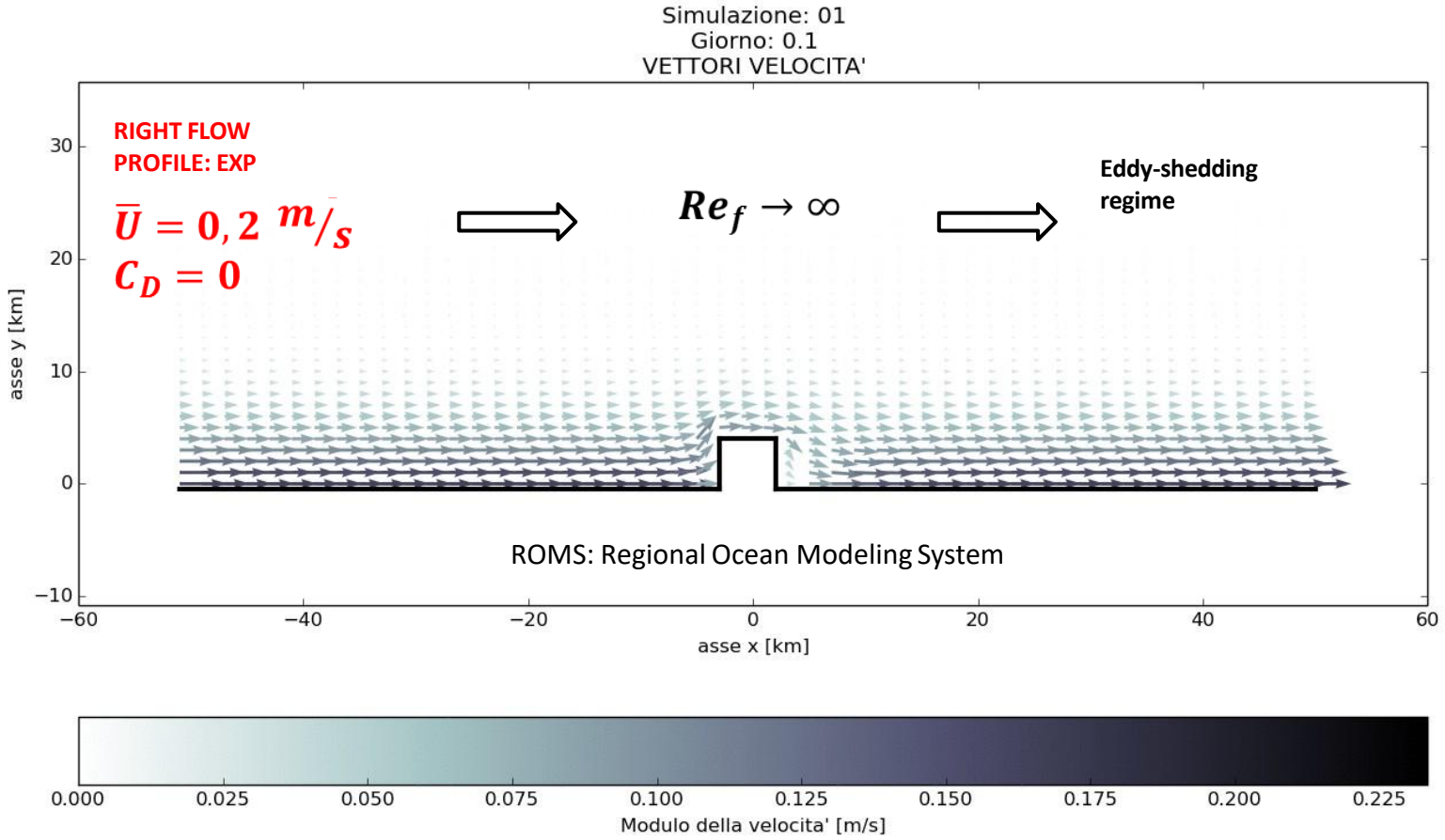

Current direction and square capes

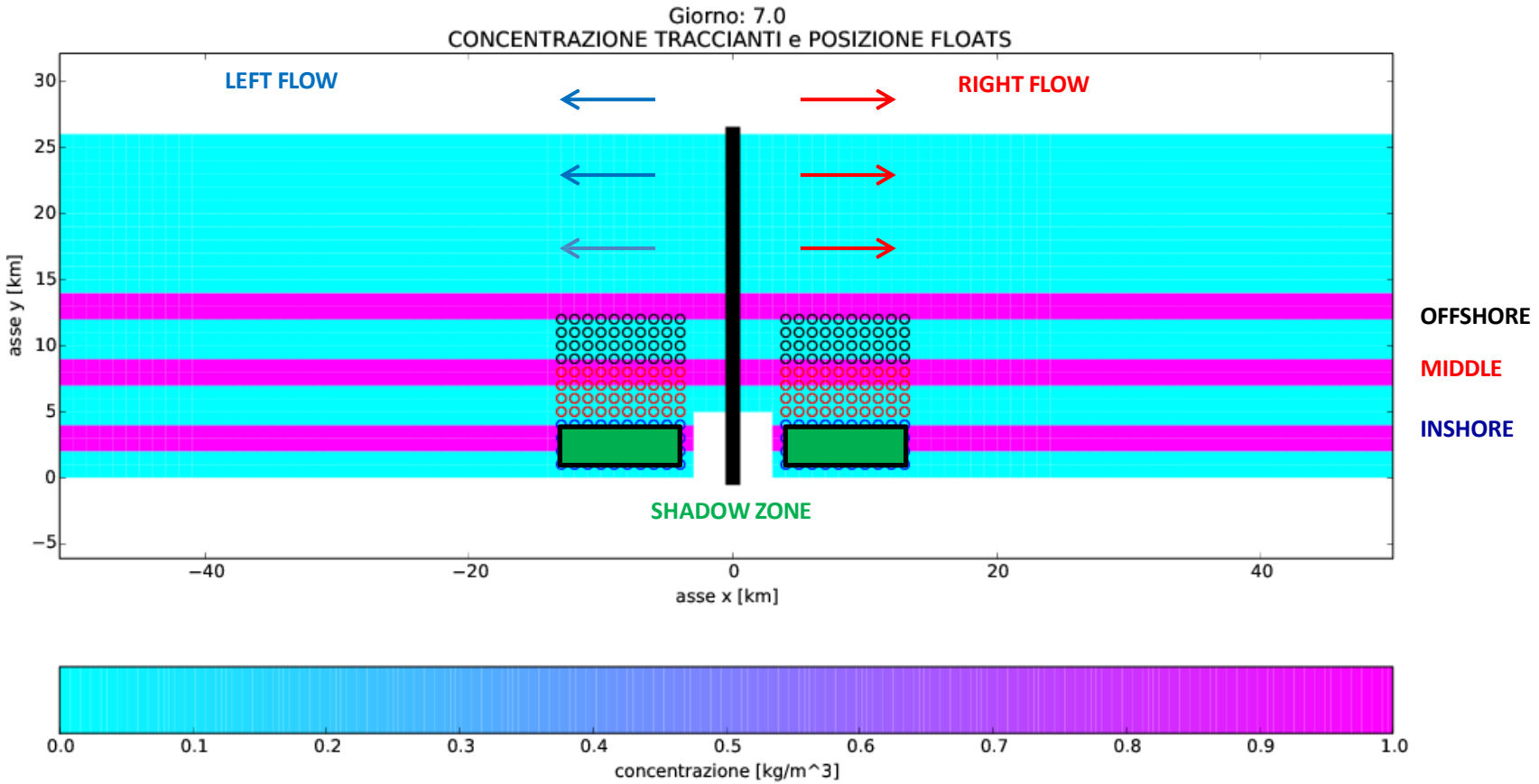

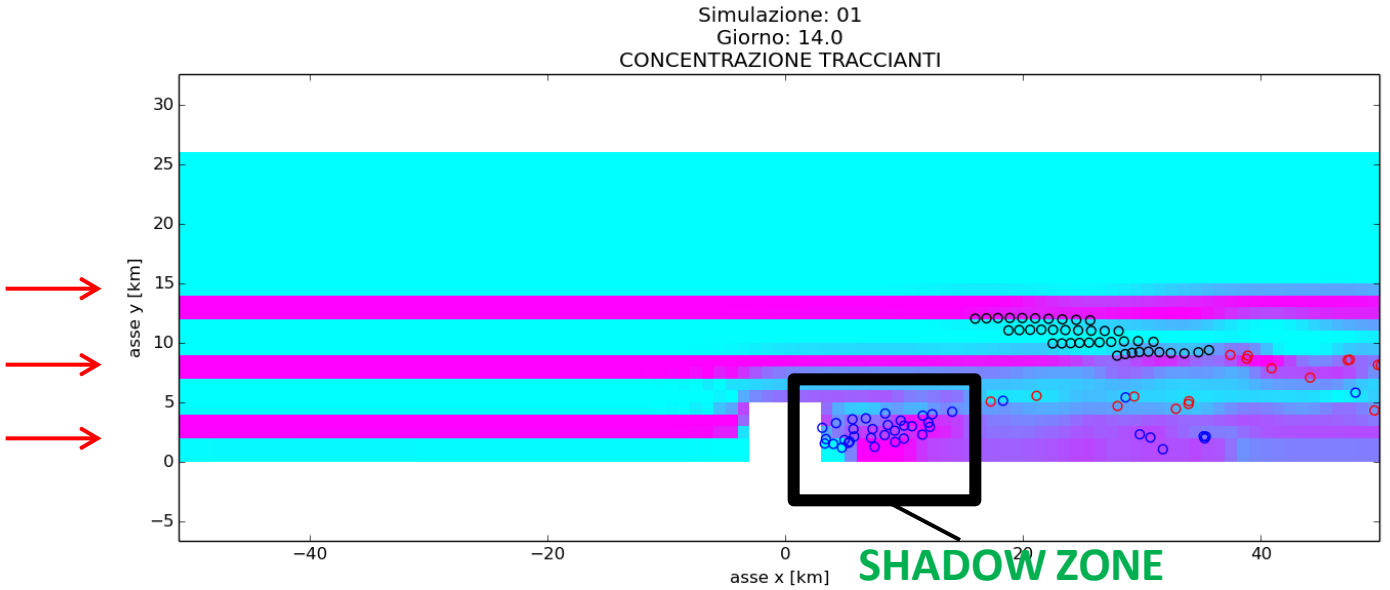

RIGHT FLOW

PROFILE: *exp*

$\bar{U} = 0,2\ m/s$

$C_D = 0$

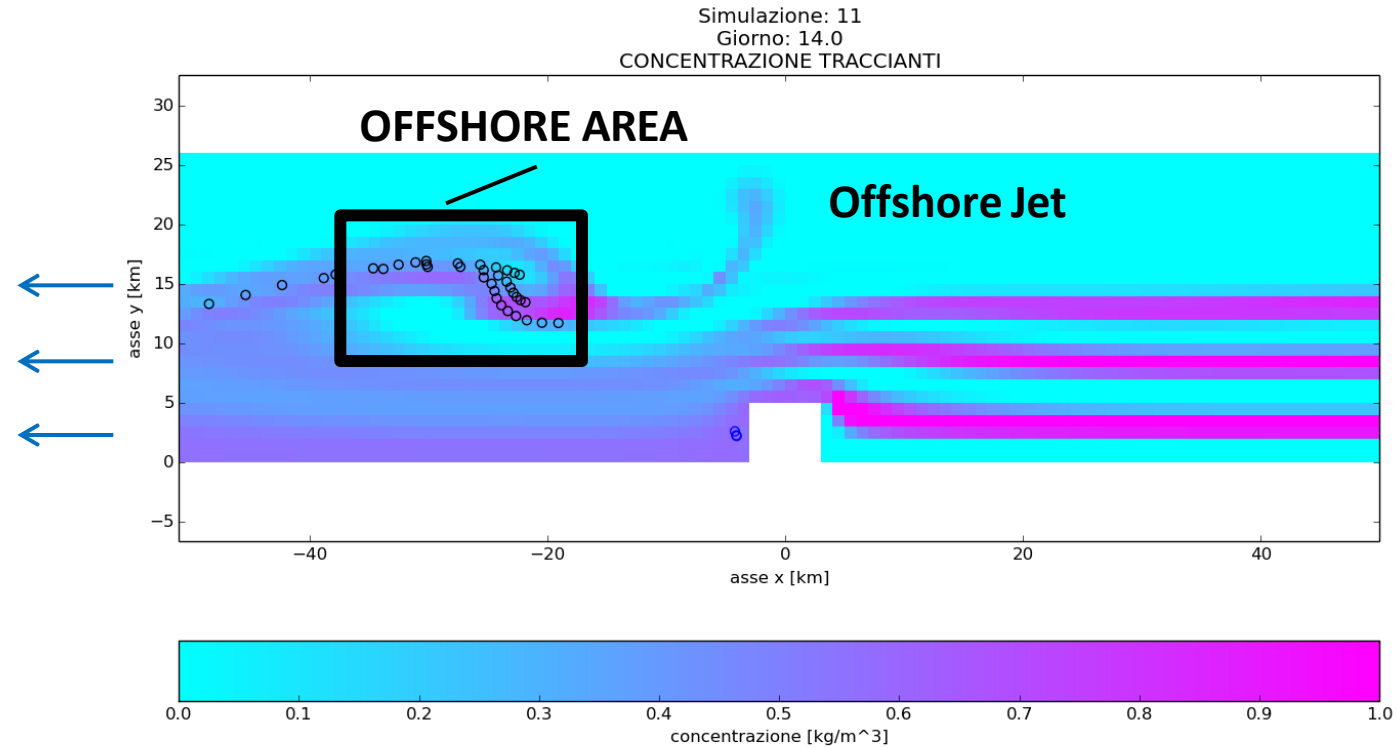

LEFT FLOW

PROFILE: *exp*

$\bar{U} = 0,5\ m/s$

$C_D = 0$

Topographic Rossby waves

POTENTIAL VORTICITY CONSERVATION

$$\frac{\partial Q}{\partial t} = 0$$

$$Q = \frac{(f + \zeta)}{H}$$

$$f = cost.$$

$$\zeta = \frac{\partial v}{\partial x} - \frac{\partial u}{\partial y}$$

$$\frac{\partial H}{\partial y} > 0$$

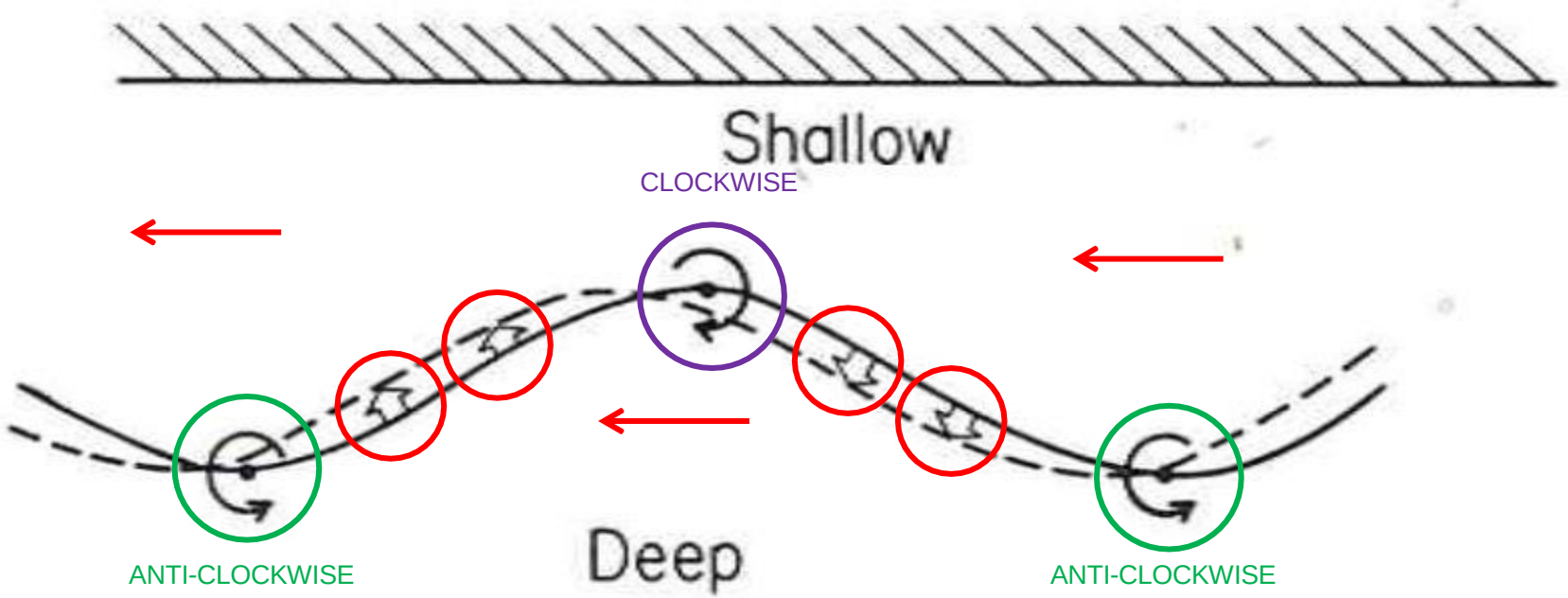

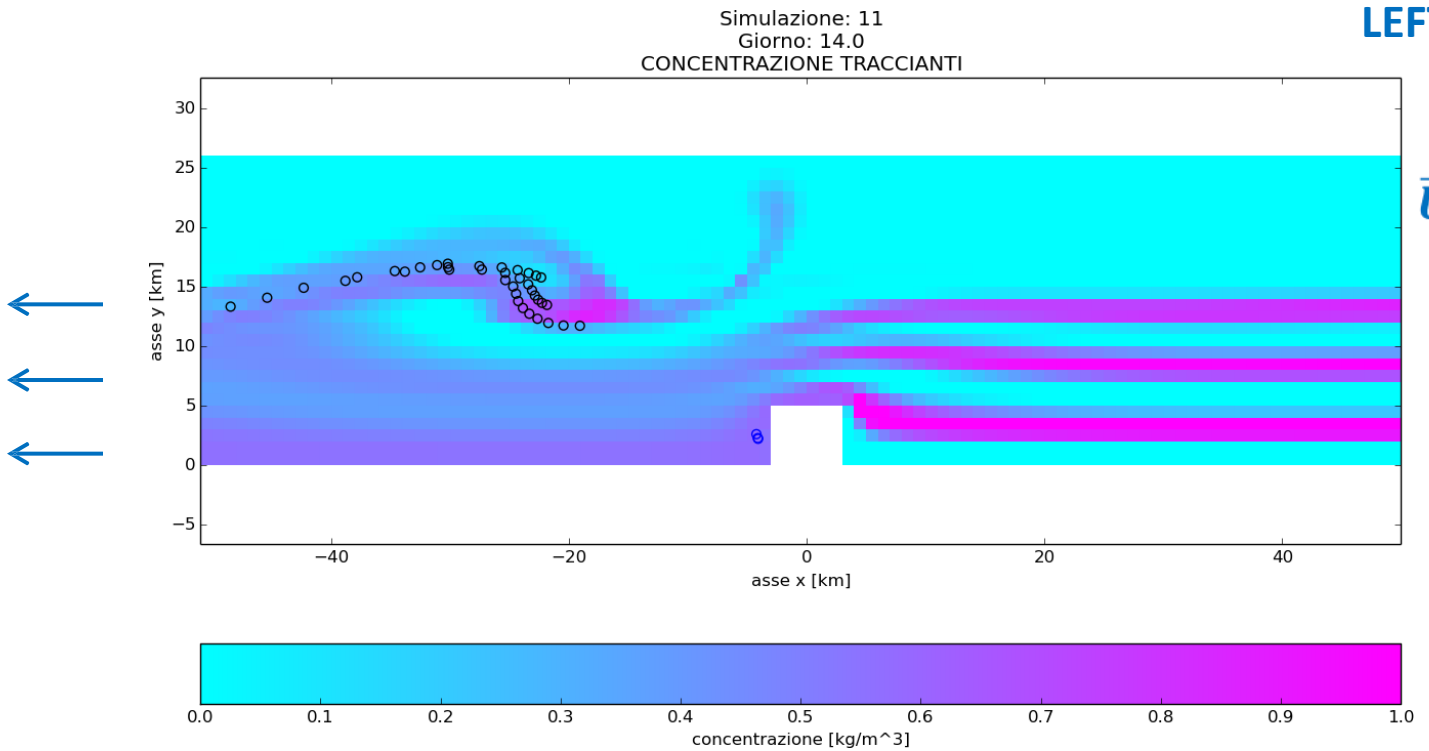

LEFT FLOW

PROFILE: *exp*

$\bar{U} = 0,5\ {}^{m}/_{s}$

$C_D = 0$

Quantification

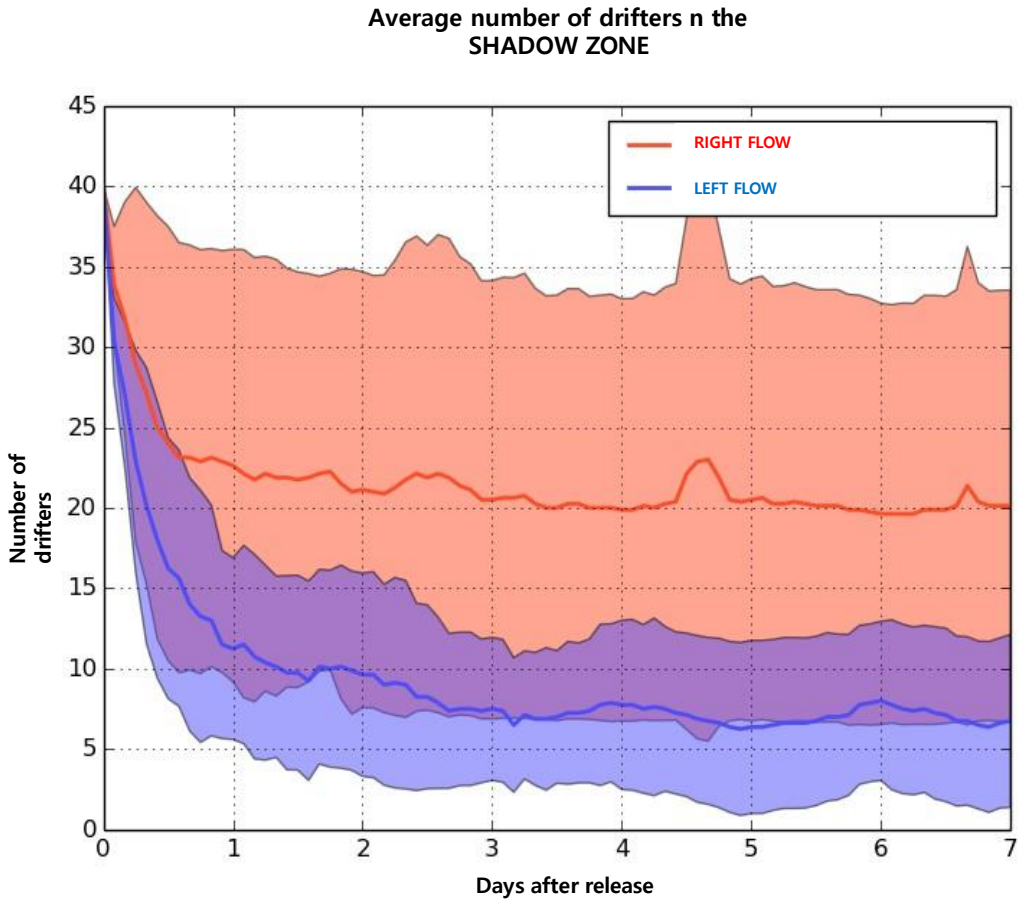

20
50%

7
17,5%

RIGHT FLOW:
Half of the synthetic drifters remains in the SHADOW ZONE after 7 days

LEFT FLOW:
Absolute dispersion is on average **20 km** larger

$$D_{abs}(t) = 1/M \sum_{m=1}^{M} \sqrt{[x_m(t) - x_m(0)]^2 + [y_m(t) - y_m(0)]^2}$$

Red gorgonian

Paramuricea Clavata

A sessile benthic species that lives throughout the Mediterranean, especially on the Ligurian/Tuscan shelf

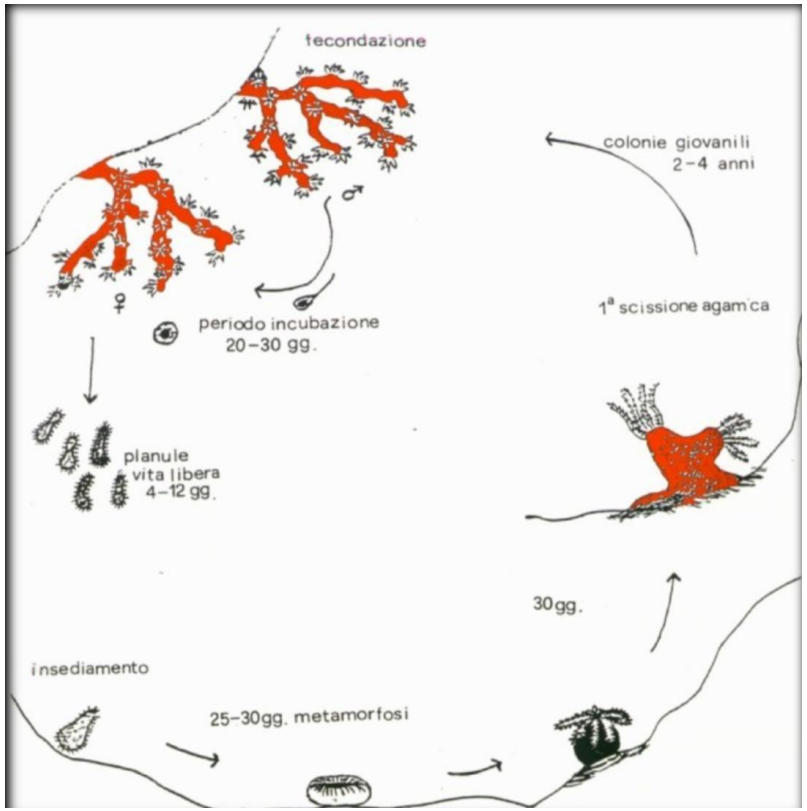

- Colonies spawn annually at the onset of warmer temperatures
- Larvae released into the water column
- Pelagic larval duration (PLD) of 4-21 days
- Larvae settle on rocky substrates and slopes at depths ~ 30m

Gene flow

Gene flow analysis (spread of genes among gorgonian populations) shows both retention (white portion of the pie chart) and connectivity (coloured portion of the pie chart)

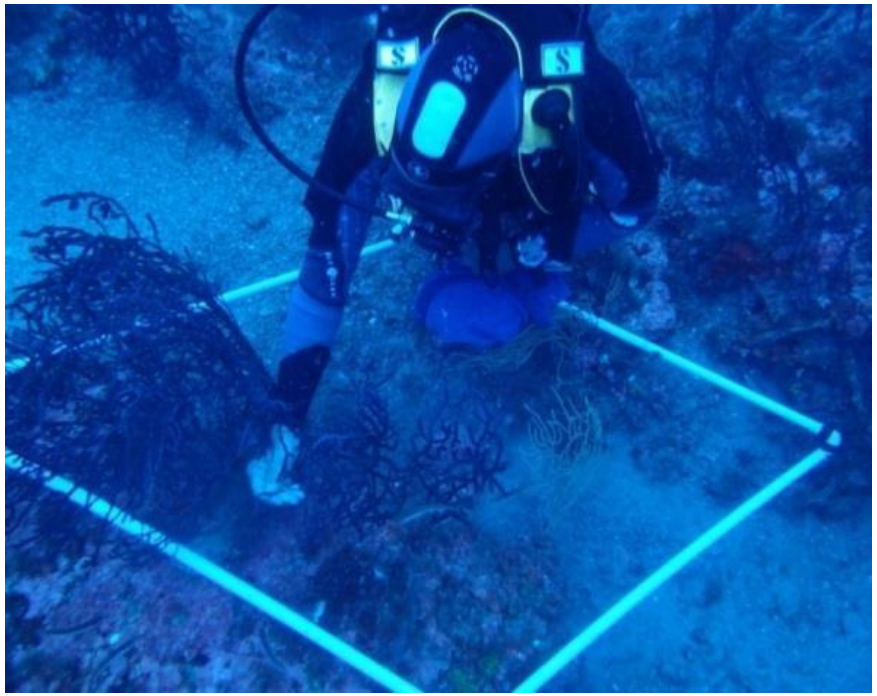

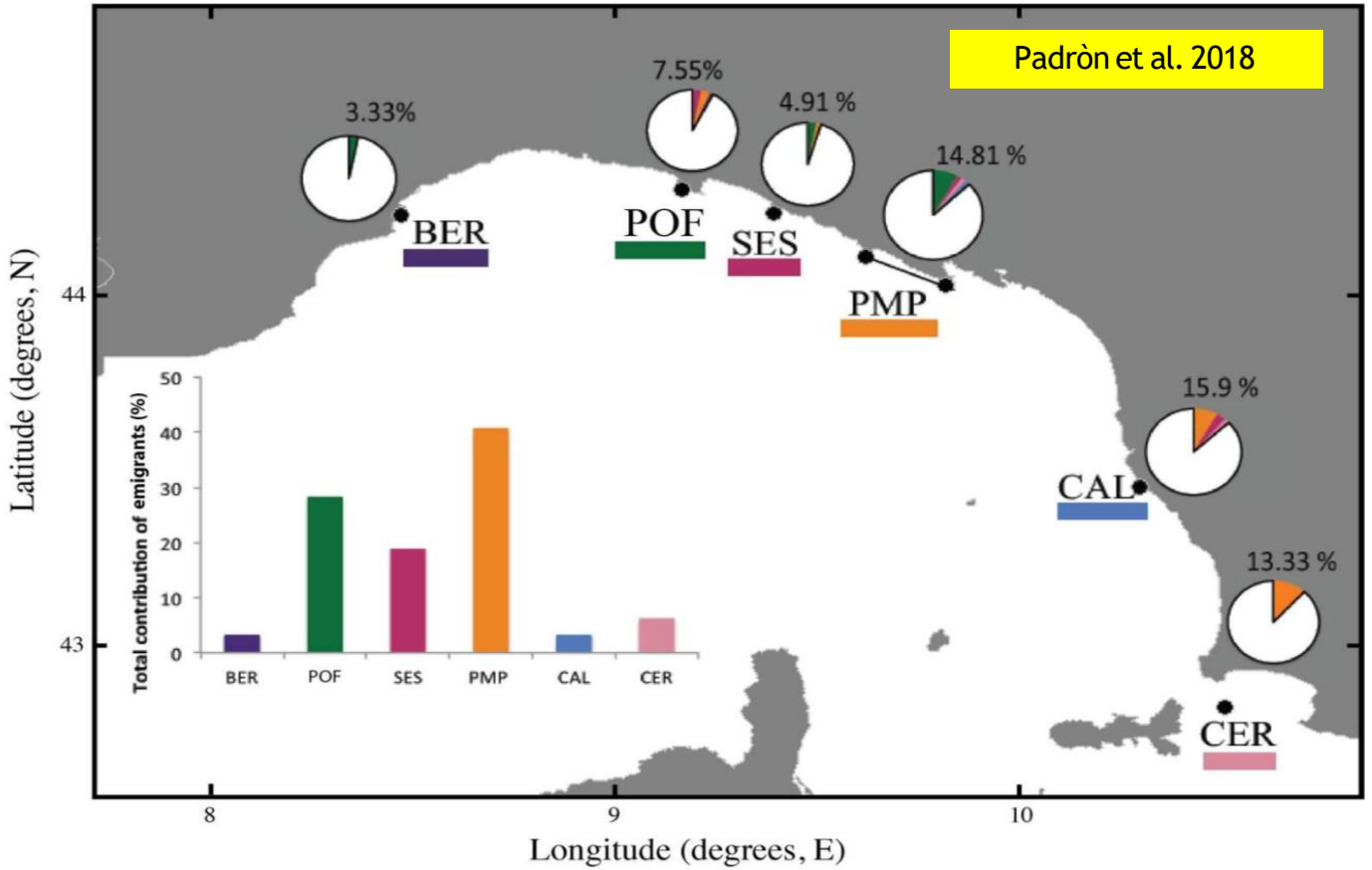

Lagrangian simulations and connectivity

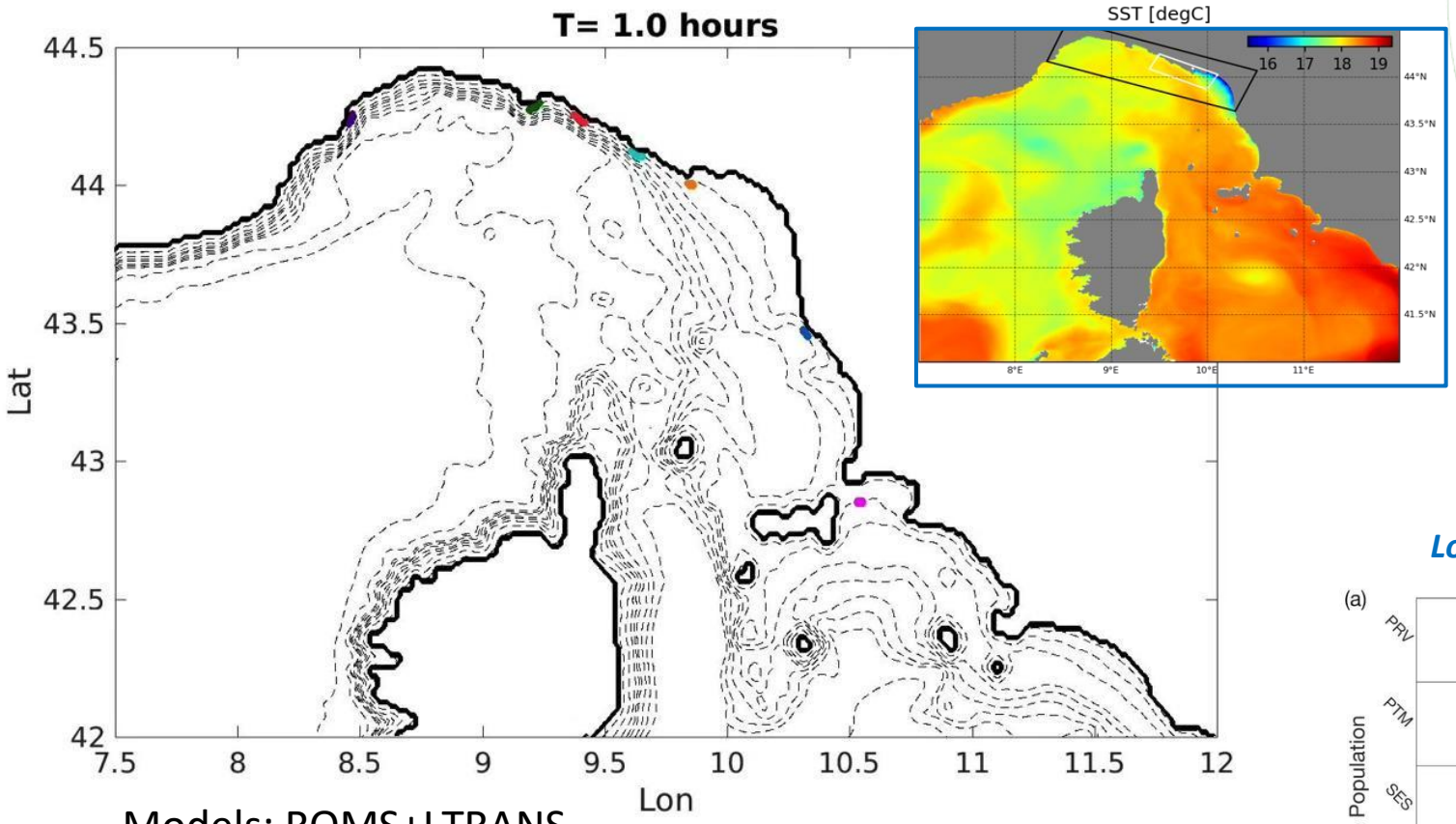

Models: ROMS+LTRANS

- Isolation of Bergeggi
- Importance for the connectivity of populations in the centre of the Ligurian Sea

Sciascia et al, 2022, ICES J. Mar. Sci.

Horizontal resolution is the most influential factor on connectivity

Low-res. ROMS 1.2 km

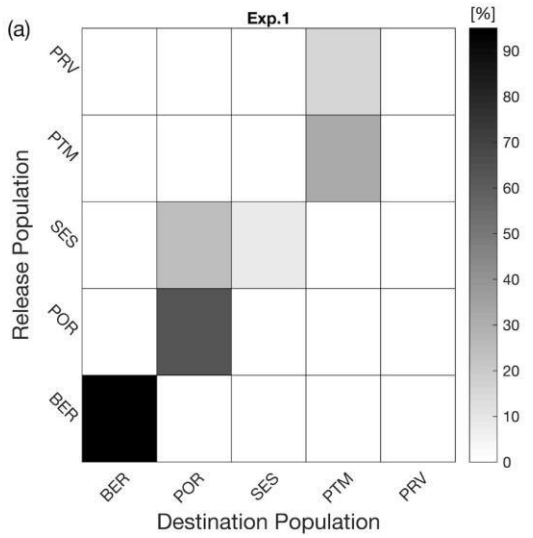

High-res. MITgcm 0.3 km

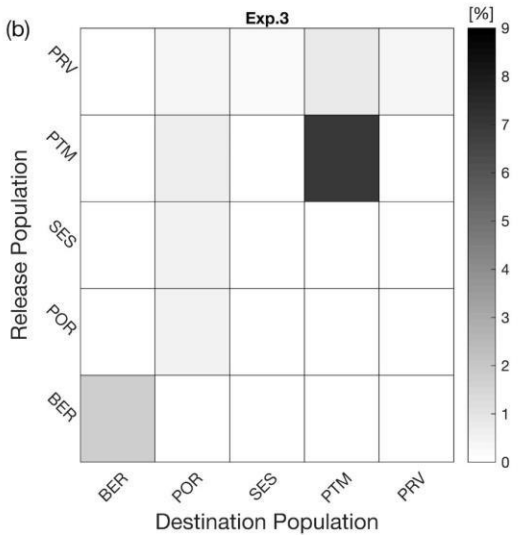

LAgrangian Variational Analysis

Black color: trajectories of the independent drifters, not used in LAVA

Green color: trajectories *WITHOUT* LAVA

Magenta color: trajectories *AFTER* LAVA correction

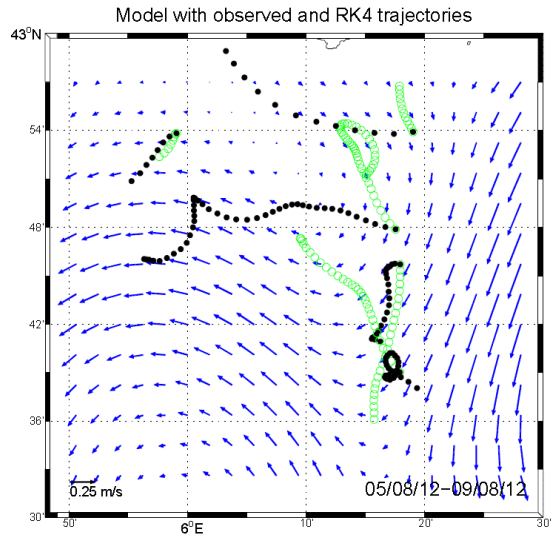

(c)

LAVA: quantitative results

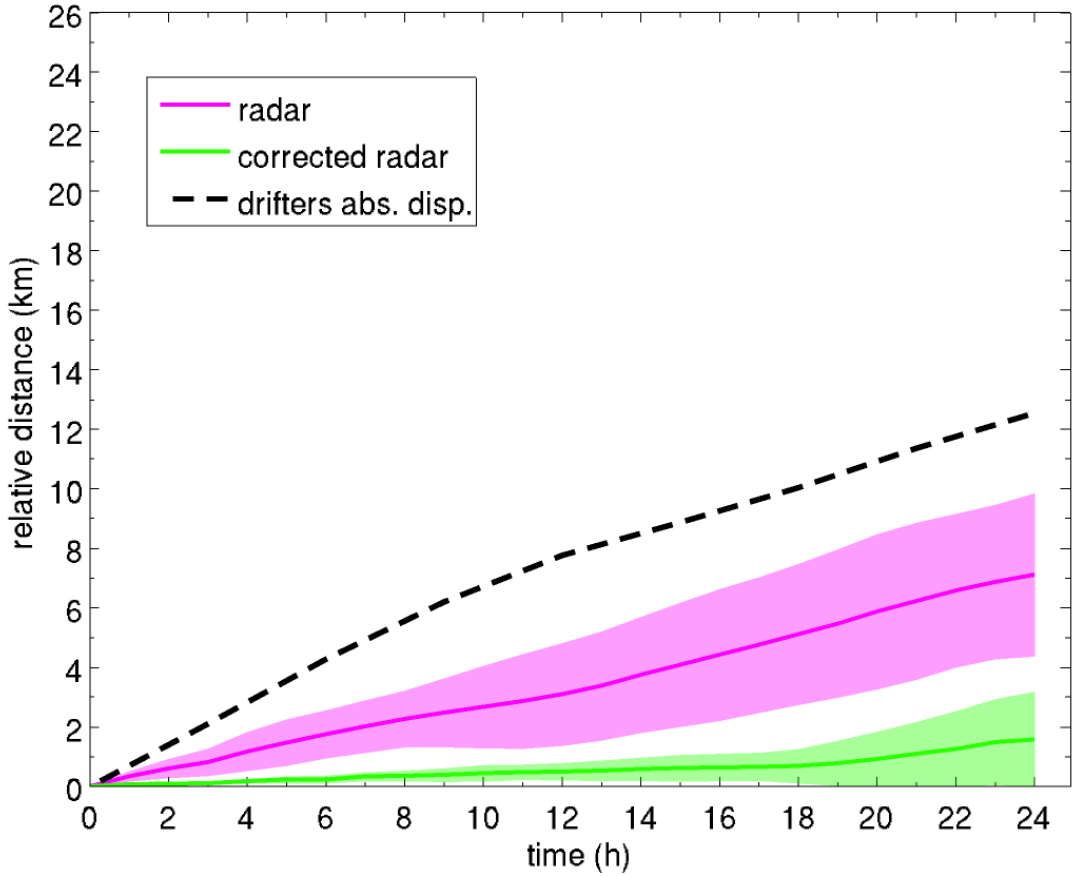

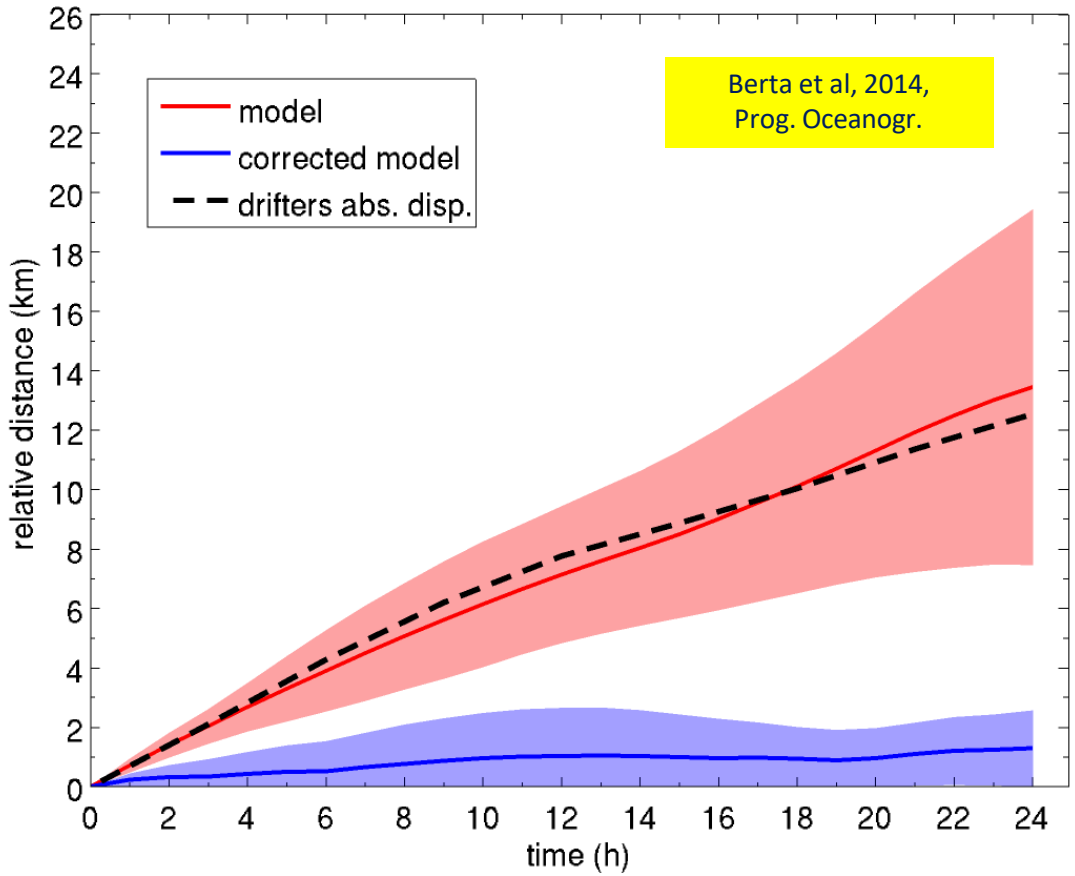

Berta et al, 2014, Prog. Oceanogr.

- Without LAVA, radars provide acceptable dispersion estimates, with an average error of about 5km after 24h. The errors for the model are larger, 10-12km after 24h
- LAVA significantly improves both radar and model estimates, with average errors decreasing to about 2km after 24h

LAVA in the Gulf of Mexico

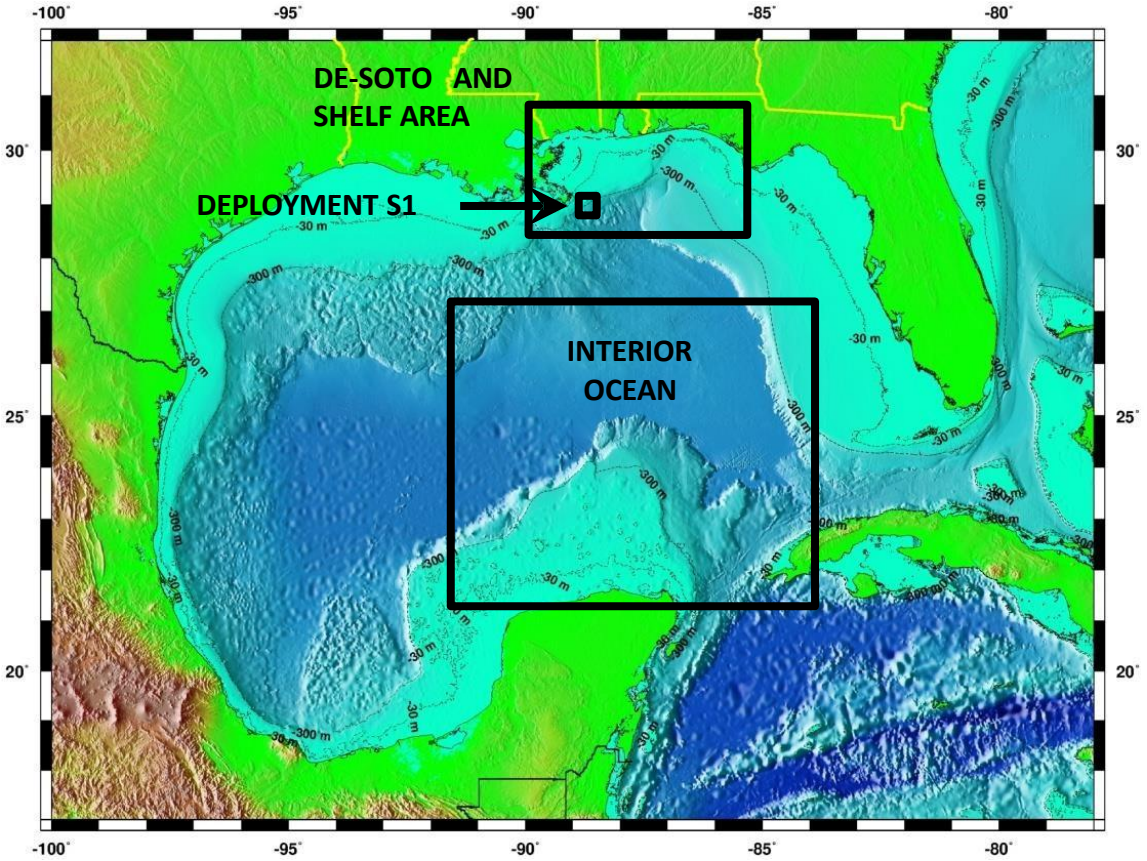

Example of trajectories used (in red) and not used (in black) by LAVA

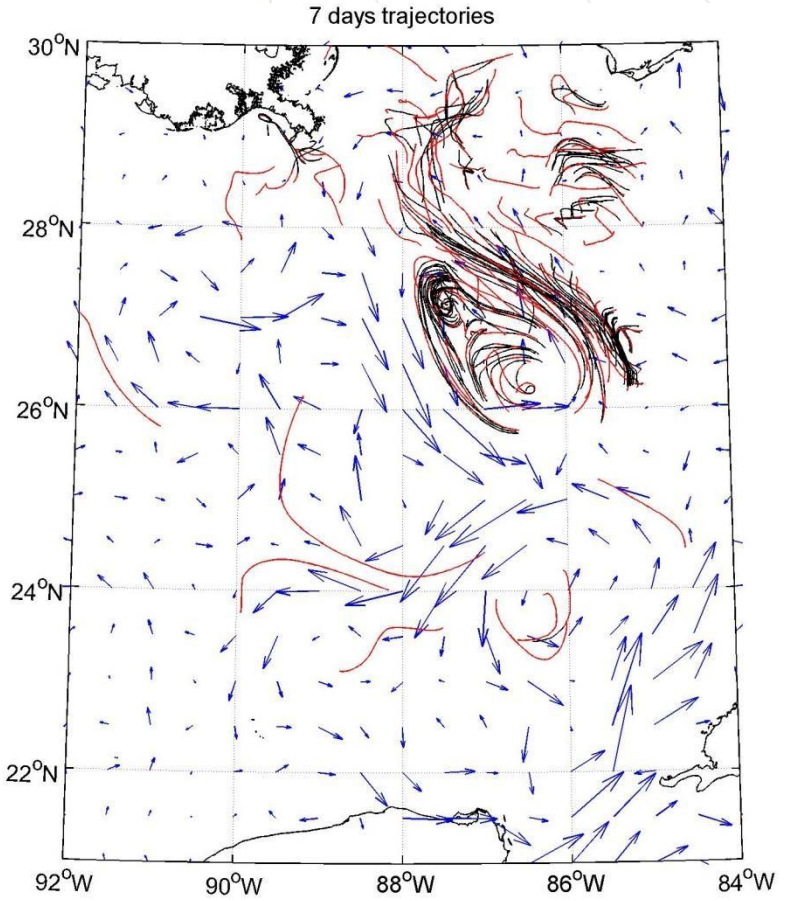

Eulerian field: AVISO satellite geostrophic velocities (in blue)

Berta et al, 2015, J. Atmos. Ocean Tech.

Lagrangian results

Interior ocean

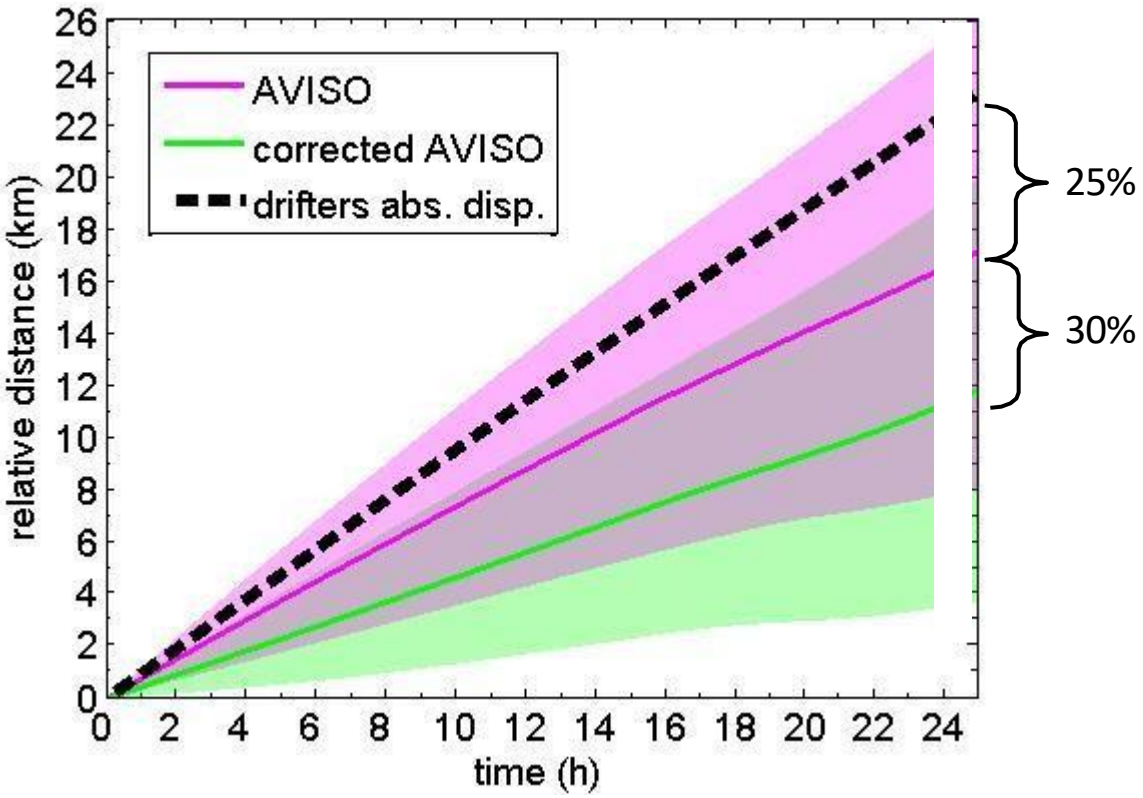

Shelf area

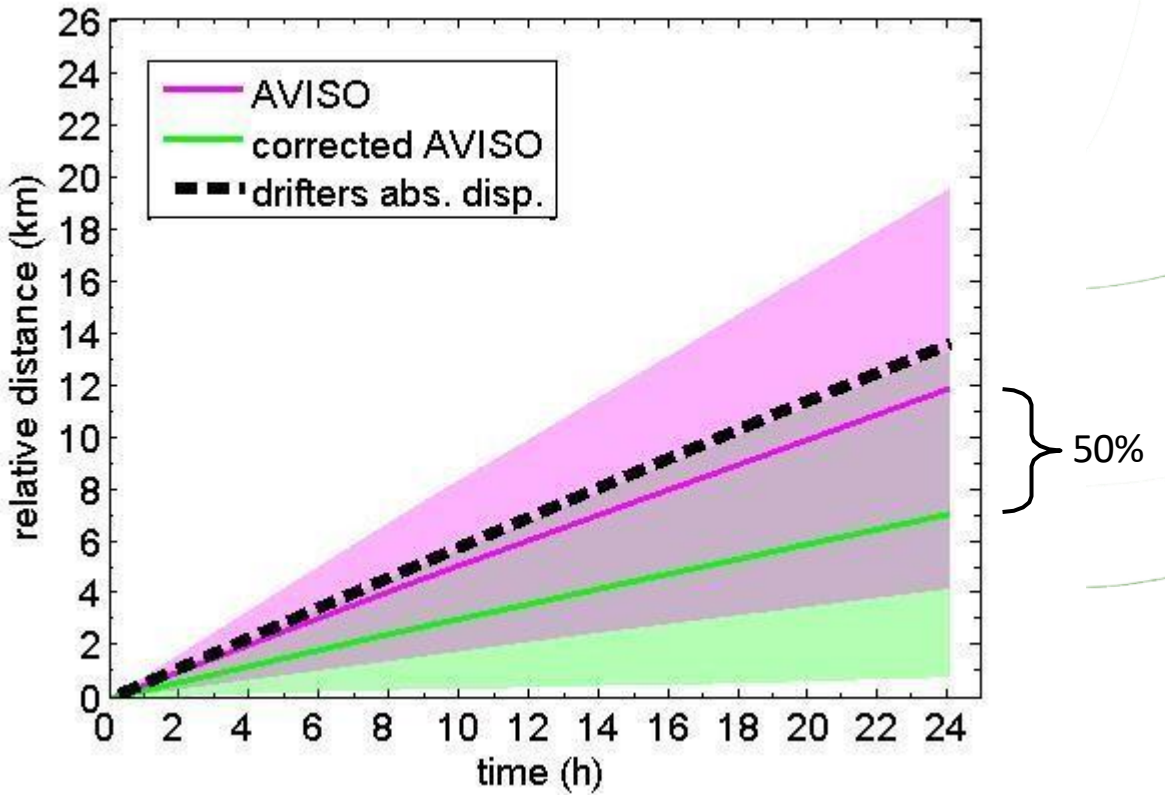

- Dispersion estimates with AVISO currents are acceptable in the deep ocean
- LAVA significantly improves results in both deep ocean and coastal areas

Conclusions

- Marine currents are highly variable in space and time when we deal with the time scale of current interest. Much more Mafalda than Naomi.
- Marine RIs are fundamental to resolve such a variability
- The multiplatform approach should be the target to better resolve the 4D complexity of the marine dynamical processes (coalescence of marine RIs)
- Ocean models should be part of the observational effort: integrated observing systems as already done in some RIs (e.g. DANUBIUS)


VOGUE
MAR
2022

THANKS!

IR0000032 – ITINERIS, Italian Integrated Environmental Research Infrastructures System
(D.D. n. 130/2022 - CUP B53C22002150006) Funded by EU - Next Generation EU PNRR-Mission 4 “Education and Research” - Component 2: “From research to business” - Investment 3.1: “Fund for the realisation of an integrated system of research and innovation infrastructures”

Finanziato dall'Unione europea NextGenerationEU
Ministero dell'Università e della Ricerca
Italiadomani

Lagrangian and Eulerian viewpoints

http://www.flowillustrator.com

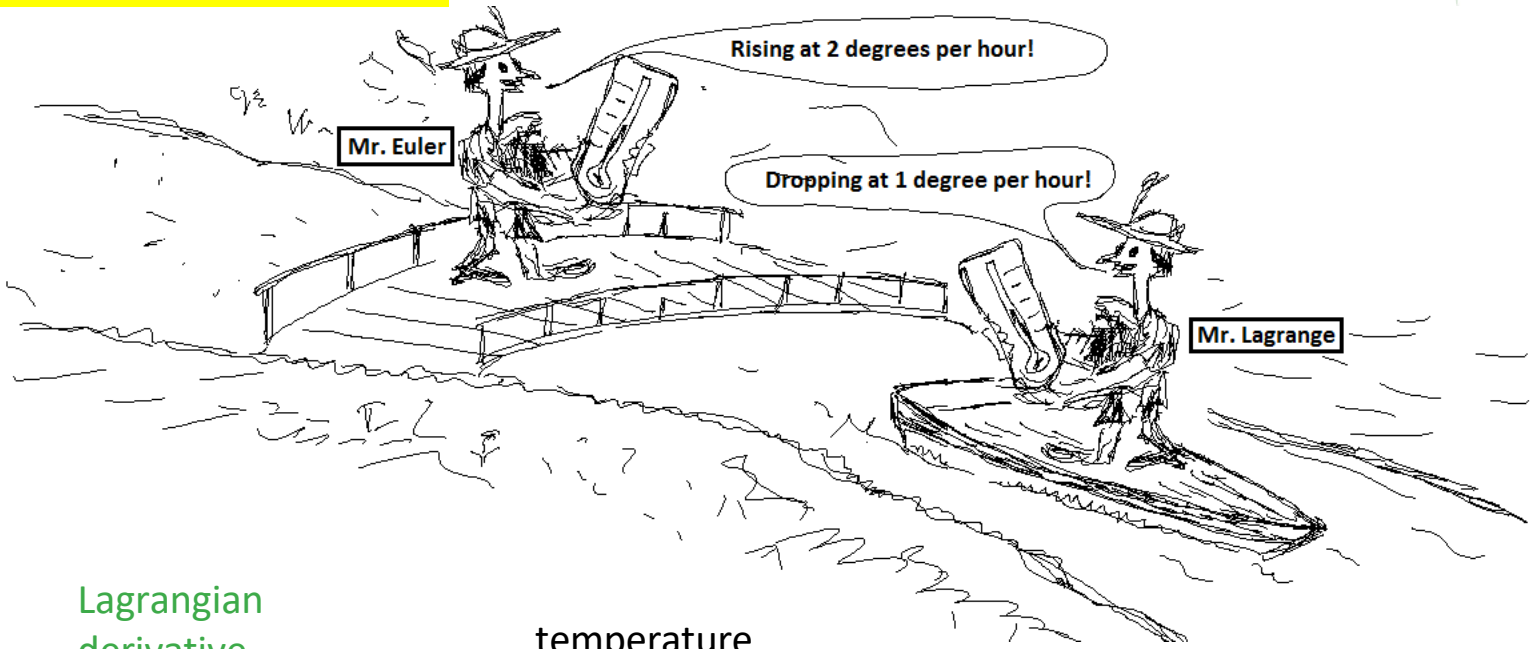

Lagrangian derivative

temperature

velocity

$$\frac{dT}{dt} = \frac{\partial T}{\partial t} + \vec{u} \cdot \vec{\nabla} T$$

time

Eulerian derivative

The Eulerian viewpoint consists in considering quantities as dependent on time and point in space

The Lagrangian viewpoint consists in considering quantities as dependent on time and moving with a fluid particle

Mr. Euler is standing on a bridge measuring temperatures carried by different particles passing through that specific point at different times

Mr. Lagrange is moving with the fluid and measuring the particles' temperature as they change in time

Their rates of change (derivatives) are different